UNIVERSITY OF CALIFORNIA,
IRVINE

Two new approaches for electronic structure: Partition Density Functional Theory and Potential Functional Theory

DISSERTATION

submitted in partial satisfaction of the requirements
for the degree of

DOCTOR OF PHILOSOPHY

in Physics

by

Peter A Elliott

Dissertation Committee:
Professor Kieron Burke, Chair
Professor Ruqian Wu
Professor Craig Martens

2009

The dissertation of Peter A Elliott
is approved and is acceptable in quality and form for
publication on microfilm and in digital formats:

_____

_____

_____

Committee Chair

University of California, Irvine
2009

TABLE OF CONTENTS

LIST OF FIGURES

LIST OF TABLES

ACKNOWLEDGMENTS

I would like to thank...

Mum, Dad, Alan, Nana

Ciarán Bourke

Co-authors Adam and Morrel.

Burke group, past and present. Theo chem students.

Dave, Hugo, John, Ruairi, Shane, Aoife, Fiona, Jim, Mike, Donghyung, Attila, Christoph, Dmitrij, Ingolf

NSF: CHE-0809859

Acknowledge copyright - APS, JCTC, CJC

CURRICULUM VITAE

Peter A Elliott

EDUCATION

Doctor of Philosophy in Physics **2009**
University of California, Irvine *Irvine, California*

Master of Physics **2006**
Rutgers, The State University of New Jersey *New Brunswick, New Jersey*

Bachelor of Arts in Theoretical Physics **2004**
Trinity College Dublin *Dublin, Ireland*

TEACHING EXPERIENCE

Fall 04 - Lab Instructor - Elements of Physics (for Pharmacists)
Spring 05 - Recitation Instructor - Analytical Physics II
Summer 05 - Recitation Instructor - General Physics
Fall 05 - Course Administrator & Lab Instructor - Elements of Physics
Spring 06 - Lab Instructor - General Physics Lab

CONFERENCES AND PRESENTATIONS

- - Time-Dependent Density Functional Theory: Prospects and Applications, 2nd International Workshop and School, Benasque, Spain, September 2005
- **Poster** - *Semiclassical Origins of Density Functionals* - Time-Dependent Density Functional Theory Gordon Research Conference, July 2007
- **Talk** - *Semiclassical Approaches in Density Functional* - American Physical Society March Meeting 2008
- **Poster** - *Time-dependent density functional theory for plasmonics* - ISIS poster session June 13, 2008, and CASTL NSF site visit
- **Talk** - *Density Functional Theory and Semiclassical Methods* - American Physical Society March Meeting 2009
- **Poster** - *Partition Density Functional Theory* - From Basic Concepts to Real Materials, KITP Santa Barbara, November 2009

PUBLICATIONS

1. *Semiclassical origins of density functionals*, P. Elliott, D. Lee, A. Cangi, and K. Burke, Phys. Rev. Lett. **100**, 256406 (2008).

2. *Excited states from time-dependent density functional theory*, P. Elliott, F. Furche, and K. Burke, in *Reviews in Computational Chemistry, Volume 26*, eds. K. B. Lipkowitz and T. R. Cundari (Wiley-VCH, New York 2008), pp 91-165.

3. *Density functional partition theory with fractional occupations*, P. Elliott, M. H. Cohen, A. Wasserman and K. Burke, J. Chem. Theory Comput. **5**, 827 (2009).

4. *Non-empirical 'derivation' of B88 exchange functional*, P. Elliott and K. Burke, Can. J. Chem. **87**, 1485 (2009).

5. *Partition Density Functional Theory*, P. Elliott, M.H. Cohen, A. Wasserman, K. Burke, submitted. Also arXiv:0901.0942 (2009).

6. *Potential scaling in density functional theory*, P. Elliott and K. Burke, in prep. Previous version: arXiv: 0906.0340 (2009).

SELECTED HONORS AND AWARDS

Gold Medal **2004**
Trinity College Dublin

ABSTRACT OF THE DISSERTATION

Two new approaches for electronic structure:
Partition Density Functional Theory and Potential Functional Theory

By

Peter A Elliott

Doctor of Philosophy in Physics

University of California, Irvine, 2009

Professor Kieron Burke, Chair

In this work I discuss two new approaches to the electronic structure problem. Both these approaches share the same goal of making electronic structure calculations faster and more accurate and both involve the popular electronic structure method of density functional theory (DFT). The first is potential functional theory which makes use of semiclassical methods to understand and improve density functional theory. In particular it explains why local approximations in DFT work as well as they do and why the generalized gradient approximations developed in the late 1980's, early 1990's were needed at all. I also develop direct potential functional approximations for the density and kinetic energy density for particles in an arbitrary potential with hard walls. As such they avoid solving the difficult Schrödinger's equation. I demonstrate their accuracy on a simple system. The second is partition density functional theory (PDFT) which solves for molecular properties while only requiring calculations on smaller fragments. This would greatly speed up computations and allow much large systems to be studied. I give a detailed derivation of PDFT before demonstrating its formal exactness on three types of system. Both these approaches have the potential to cure some of the problems DFT suffers from and these possible consequences are discussed.

Chapter 1

Introduction

The goal of electronic structure to be able to understand and predict the behavior of a wide range of materials, be they atoms, molecules, clusters, or solids. It specifically deals with the ground state of the electrons in the system, however knowledge of this also provides a great deal of other information (such as the ground state geometry).

From a certain perspective, this problem is already solved. The solution of Schrödinger's equation in quantum mechanics within the Born-Oppenheimer approximation gives us exactly the information we seek. Unfortunately, to solve the problem exactly is essentially impossible if you wish to study systems with 1000's of electrons, even 2 electrons can be a very hard problem to solve exactly. This is due to the interaction between the electrons being extremely difficult to handle. So the problem becomes to solve the Schrödinger equation without actually solving the Schrödinger equation. Many different approaches for solving this problem have been developed, each one has advantages and disadvantages usually involving a trade off between accuracy and computational efficiency.

Density functional theory (DFT) is one such method that has become popular. It

maps the interacting problem to that of a non-interacting system which may be solved much more easily. It is based upon the rigorous theorem of Hohenberg-Kohn[1] and the scheme of Kohn and Sham[2]. DFT requires an approximation to an unknown quantity named the exchange-correlation energy, however there are now many approximations that work well enough for chemical applications. In fact there is a plethora of such exchange-correlation approxiamtions, due to the fact that there is no systematic way to approach its approximation. The simplest of these is a local density approximation which works far better than one would expect given its simplicity. Despite working with non-interacting fermions, DFT still scales with roughly the cube of the system size and eventually becomes computationally too expensive for large systems.

Semiclassical methods lie somewhere inbetween the non-intuitive nano-scale world of quantum mechanics and the classical Newtonian world of everyday live. These methds are also a way to avoid solving the Schrödinger equation directly giving approximations that will become exact in certain limits. The $\hbar \to 0$ limit is commonly called the semiclassical limit.

In this work, I explore two new methods for solving the electronic structure problem. In both cases, the goal is to be more accurate and more efficient. In the first, semiclassical methods are used to develop approximations to the density and kinetic energy density as functionals of the potential. These can then be analyzed from the perspective of DFT and shed new light on why DFT works. In particular it answers why local approximations work so well and why the so called generalized gradient approximations needed to be developed ontop of the simple gradient corrections. This work not only has the potential to improve DFT but also to become a distinct electronic structure method in its own right. The second method is partition density functional theory (PDFT) which solves for molecular properties while only requiring

calculations on smaller fragments. This would greatly speed up computations and allow much large systems to be studied, as it, in principle, scales linearly with system size.

This dissertation is organized as follows: first I give the relevant background information on quantum mechanics, semiclassical methods and finally DFT (including a detailed look at the generalized gradient approximations (GGAs)). Next is the potential functional theory section dealing with semiclassical methods and DFT. It includes the derivation of potential functionals for the density and kinetic energy density for a simple system as well as detailed analysis into what DFT misses and in the case of the GGAs, why they have to be made the way they are. Then we move to PDFT, which is introduced via partition theory, before being rigorous derived and investigated, and then demonstrated on a series of system. Lastly I conclude with a detailed overview of the results for each approach followed by a discussion on how they may influence eachother.

Chapter 2

Background

In this chapter, we review the relevant background in semiclassical methods and density functional theory.

2.1 Quantum Mechanics

I start this chapter with quantum mechanics so that the problem of electronic structure discussed in later chapters is well defined. I shall be extremely brief as quantum mechanics is taught at the undergraduate level. We begin with the time-independent Schrödinger equation[3]:

$$\hat{H}\psi = E\psi \tag{2.1}$$

The Hamiltonian at this stage contains both the nuclei and the electrons that make up a given piece of matter. We next make the Born-Oppenheimer approximation that separates the nuclear and electronic degrees of freedom, and we concentrate on the

electronic Hamiltonian defined by

$$\left[\hat{T} + \hat{V}_{\text{ee}} + \hat{V}_{\text{ext}}\right] \psi = E\psi \tag{2.2}$$

where $\hat{T}$ is the kinetic energy of the electrons, $\hat{V}_{\text{ext}}$ is the electron-nuclear interaction defined explicitly below, and $\hat{V}_{\text{ee}}$ is the coulomb interaction between the electrons. In co-ordinate space, this is written as

$$\left[-\frac{\hbar^2}{2m}\sum_{\alpha=1}^{N}\nabla_\alpha^2 + \frac{1}{2}\sum_{\alpha=1}^{N}\sum_{\beta\neq\alpha}^{N}\frac{e^2}{|\mathbf{r}_\alpha - \mathbf{r}_\beta|} + \sum_{\alpha=1}^{N} v_{\text{ext}}(\mathbf{r}_\alpha)\right]\psi(\mathbf{r}_1, ..., \mathbf{r}_N) = E\psi(\mathbf{r}_1, ..., \mathbf{r}_N) \tag{2.3}$$

for N electrons. The external potential is

$$v_{\text{ext}}(\mathbf{r}) = \sum_{a=1}^{M}\frac{-Z_a}{|\mathbf{r} - \mathbf{R}_a|} \tag{2.4}$$

which is the coulomb potential from M nuclei with atomic numbers $\{Z_a\}$ at positions $\{\mathbf{R}_a\}$. We will not deal with electric or magnetic fields. The probability to find any electron at a point $\mathbf{r}$ is given by the density of the system as defined by

$$n(\mathbf{r}) = N\int d^3r_2 \ldots \int d^3r_N |\psi(\mathbf{r}, \mathbf{r}_2, \ldots, \mathbf{r}_N)|2 \tag{2.5}$$

This them defines the electronic structure problem. We wish to find the ground state energy for a given number of electrons in a given external potential.

In all the numerical examples that appear later, we will work with non-interacting fermions in one dimension. The non-interacting Schrödinger equation for this case is

$$\left[-\frac{\hbar^2}{2m}\partial_x^2 + v_{\text{ext}}(x)\right]\phi_j(x) = \epsilon_j\phi_j(x) \tag{2.6}$$

where $\partial_x^2 = d^2/dx^2$ and the density is given by

$$n(x) = \sum_{j=1}^{N} |\phi_j(x)|^2 \tag{2.7}$$

2.2 Green's function

Very closely related to Schrödigner's equation is the Green's function. For non-interacting fermions in 1d, the Green's function satisfies the equation

$$\left(-\frac{\hbar^2}{2m}\partial_x^2 + v_{\text{ext}}(x) - E\right) G(x, x'; E) = -\delta(x - x') \tag{2.8}$$

with the appropriate boundary conditions. The Green's function can be written in terms of the eigenfunctions from Eq. (2.6)

$$G(x, x'; E) = \sum_j \frac{\psi_j(x)\psi_j(x')}{E - \epsilon_j} \tag{2.9}$$

where $\psi_j(x)$ is chosen to be real in this equation. The density of the system can be written as

$$n(x) = \frac{1}{2\pi i} \oint_C dE\ G(x; E) \tag{2.10}$$

where $G(x; E) = G(x, x; E)$ and the contour C crosses the real energy axis at the fermi energy E_{F}.

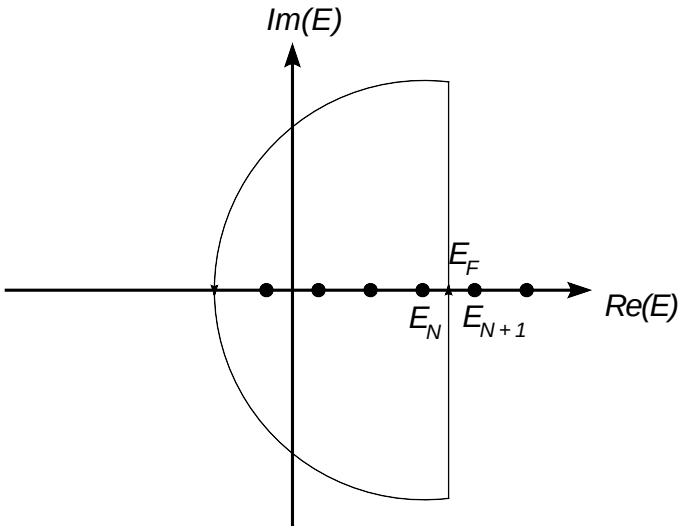

Figure 2.1: Contour in the complex energy plane that crosses the real axis at the fermi energy.

In 1 dimension, a different form for $G(x, x'; E)$ may be used

$$\begin{aligned} G(x, x'; E) &= \frac{\psi_1(x; E)\psi_2(x'; E)}{W(E)} \quad \text{, for} \quad x \leq x' \\ &= \frac{\psi_1(x'; E)\psi_2(x; E)}{W(E)} \quad \text{, for} \quad x \geq x' \end{aligned} \tag{2.11}$$

where $\psi_{1/2}(x; E)$ satisfy the Schrödinger equation

$$\left(-\frac{\hbar^2}{2m}\partial_x^2 + v_{\text{ext}}(x) - E\right)\psi_{1/2}(x; E) = 0 \tag{2.12}$$

with $\psi_1(x; E)$ only satisfying the left boundary condition and $\psi_2(x; E)$ the right. The Wronskian, $W(E)$, is given by

$$W(E) = \psi_1(x)\partial_x\psi_2(x) - \psi_2(x)\partial_x\psi_1(x) \tag{2.13}$$

2.3 Semiclassical Methods

Semiclassical methods exist in the world between the quantum mechanics of the very small scale and the classical newtonian mechanics of everyday life. The transition between these two seemingly contradicting world views is an extremely important problem in physics and has been well studied over the years[4]. We will just look at the most well-known semiclassical approximation, the Wentzel-Kramers-Brillouin-Jeffreys (WKB) approximation.

We begin by rewriting the 1-d Schrödinger equation, Eq. (2.6), as

$$\left[\hbar^2 \frac{d^2}{dx^2} + [k_j(x)]^2\right] \psi_j(x) = 0 \tag{2.14}$$

where

$$k_j(x) = \sqrt{2m(\epsilon_j - v_{\text{ext}}(x))} \tag{2.15}$$

Then we write the wavefunctin as

$$\phi(x) = e^{-iS(x)/\hbar} \tag{2.16}$$

and evaluate Eq. (2.14)

$$-i\hbar S''(x) - [S'(x)]^2 + [k(x)]^2 = 0 \ , \tag{2.17}$$

which is the Riccati equation. If we expand $S(x)$ in powers of $\hbar$:

$$S(x) = \sum_{n=0}^{\infty} \hbar^n S_n(x) \tag{2.18}$$

and split into even and odd powers $S(x) = S_+(x) + S_-(x)$, we find

$$S_-(x) = -\frac{i\hbar}{2}\log[S'_+(x)] \ , \tag{2.19}$$

which gives

$$\phi(x) = \frac{c}{\sqrt{S'_+(x)}} e^{-iS_+(x)/\hbar} \ . \tag{2.20}$$

If we write

$$S_+(x) = \int^x dx' \ Q_j(x') \ , \tag{2.21}$$

then the wavefunction becomes

$$\phi(x) = \frac{c}{\sqrt{Q_j(x)}} \exp[-\frac{i}{\hbar}\int^x dx' Q_j(x')] \tag{2.22}$$

Again using Eq. (2.14), we find the equation for $Q(x)$

$$\hbar^2\left(-\frac{Q''_j(x)}{2Q_j(x)} + \frac{3}{4}\left[\frac{Q'_j(x)}{Q_j(x)}\right]^2\right) - [Q_j(x)]^2 + [k_j(x)]^2 = 0 \tag{2.23}$$

where $Q(x)$ will have only even powers of $\hbar$ in its expansion. Including just the zero'th order approximation gives $Q(x) = k_j(x)$, which is the usual WKB wavefunction seen in most quantum mechanics textbooks

$$\phi_j(x) = \frac{c}{\sqrt{k_j(x)}} \exp[-\frac{i}{\hbar}\theta_j(x)] \tag{2.24}$$

where

$$\theta_j(x) = \int^x dx' \ k_j(x') \tag{2.25}$$

For a flat box with an arbitrary potential between two hard walls at $x = 0$ and $x = L$, the boundary conditions are

$$\phi_j(0) = 0 = \phi_j(L) \tag{2.26}$$

then the WKB wavefunction for this system is

$$\phi_j(x) = \frac{c}{\sqrt{k_j(x)}} \sin[\frac{1}{\hbar}\theta_j(x)] \tag{2.27}$$

which is valid when $\epsilon_j >> v(x)$. The approximation diverges at turning points, where $v_{\text{ext}}(a) = \epsilon_j$, which we will discuss later and avoid in our examples. The boundary condition give the quantization condition

$$\Theta_j = \theta_j(L) = j\pi \tag{2.28}$$

which discretizes the energy spectrum.

The WKB approximation can be systematically expanded by including more orders of $\hbar$. The next order for $Q_j(x)$ will be

$$Q_j(x) = k_j(x) + \hbar^2 Q^{(2)}(x) \tag{2.29}$$

which when inserted into Eq. (2.23) gives

$$Q^{(2)}(x) = -\frac{k_j''(x)}{4k_j^2(x)} + \frac{3}{8}\frac{\left[k_j'(x)\right]^2}{k_j^3(x)} \tag{2.30}$$

For simplicity, this can be written as

$$Q^{(2)}(x) = +\frac{v''(x)}{4k_j^3(x)} + \frac{5}{8}\frac{[v'(x)]^2}{k_j^5(x)} \tag{2.31}$$

using

$$k_j'(x) = -\frac{v'(x)}{k_j(x)} \quad , \quad k_j''(x) = -\frac{v''(x)}{k_j(x)} - \frac{[v'(x)]^2}{k_j^3(x)} \tag{2.32}$$

2.4 DFT

Density functional theory (DFT) is an extremely popular method for solving electronic structure problems in many fields, due to its balance of reasonable accuracy with computational efficiency[5]. The price you pay for this efficiency is that DFT requires an approximation to an unknown quantity, namely the exchange-correlation (XC) energy as a functional of the density. No systematic approach exists to construct these approximations, which is the reason why so many exist, and is part of the motivation for the semiclassical approach of chapter 3. I shall introduce DFT in such a way that the analogies drawn later in chapter 4 are easier to see, before going into a detailed review of generalized gradient approximations for the XC energy. For a more complete review of DFT, I recommend the *Primer in DFT*[5], *The ABC of DFT*[6] online book and the background chapter of Ref. [7]. During this review, I shall make general statements about these approximations and it is understood that more information can be found by reading these sources. Also, for simplicity everything is written for the spin-unpolarized case, thus I do not include spin labels. However the extension to spin-DFT can be found in the sources listed above, and for our purposes, everything written has a simple spin-densities equivalent.

In DFT, the Hohenberg-Kohn[1] theorem states that for a given electron-electron interaction the external potential is a unique functional of the density. Hence if the density is known, then in principle all other properties of the system are known as these are functionals of the external potential. In particular the total energy of an

interacting system can be written as a functional of the density:

$$E[n] = F[n] + V_{\text{ext}}[n] \tag{2.33}$$

where

$$V_{\text{ext}}[n] = \int d^3r\, n(\mathbf{r})\, v_{\text{ext}}(\mathbf{r}) \tag{2.34}$$

is the external potential energy and $F[n]$ is the universal functional, as defined by the Levy-Lieb constrained search over all wavefunctions Ψ yielding density $n(\mathbf{r})$:

$$F[n] = \min_{\Psi \to n(\mathbf{r})} \langle \Psi | \hat{T} + \hat{V}_{\text{ee}} | \Psi \rangle \tag{2.35}$$

where $\hat{T}$ and $\hat{V}_{\text{ee}}$ are the kinetic energy and electron-electron interaction operators respectively.

Now imagine we have solved the interacting problem, and found ground-state (gs) density $n(\mathbf{r})$, then for some perverse reason we want to know the non-interacting system for which this is the gs density of. We can apply the Hohenberg-Kohn theorem again, this time it states that there is a potential for a non-interacting system that is a unique functional of the density. We name this potential the Kohn-Sham (KS) potential $v_{\text{S}}(\mathbf{r})$. Therefore if we solve the Kohn-Sham equation[2]:

$$\left[-\frac{1}{2}\nabla_j^2 + v_{\text{S}}(\mathbf{r}) \right] \phi_j(\mathbf{r}) = \varepsilon_j \phi_j(\mathbf{r}) \tag{2.36}$$

for N non-interacting fermions in this KS potential, then the sum of the orbital densities is the exact same density as if we solved for N interacting electrons in the

external potential, i.e.

$$n(\mathbf{r}) = \sum_{j=1}^{N} |\phi_j(\mathbf{r})|^2 \tag{2.37}$$

We split the KS potential into $v_{\rm S}(\mathbf{r}) = v_{\rm ext}(\mathbf{r}) + v_{\rm HXC}(\mathbf{r})$, where $v_{\rm HXC}(\mathbf{r})$ is the extra piece added to the external potential to make the KS potential.

Now suppose we cannot solve the exact system, can we use this non-interacting system to find the exact density and energy? The answer is yes, and is done by considering all quantities as density functionals. We first define an energy $E_{\rm S}$[n]:

$$\begin{aligned} E_{\rm S}[n] &= \langle \Phi_{\rm KS}[n] | \hat{T} + \hat{V}_{\rm ext} | \Phi_{\rm KS}[n] \rangle & (2.38) \\ &= T_{\rm S}[n] + V_{\rm ext}[n] & (2.39) \end{aligned}$$

where $\Phi_{\rm KS}[n]$ is the KS wavefunction of density $n(\mathbf{r})$, and $T_{\rm S}[n]$ is the non-interacting kinetic energy. If we then define $E_{\rm HXC}[n]$ as the difference between the total system energy and this non-interacting energy:

$$E_{\rm HXC}[n] = E[n] - E_{\rm S}[n] \tag{2.40}$$

then minimization of this functional with respect to the density yields

$$v_{\rm HXC}(\mathbf{r}) = \frac{\delta E_{\rm HXC}[n]}{\delta n(\mathbf{r})} \tag{2.41}$$

as the total energy is by definition stationary and $v_{\rm HXC}(\mathbf{r}) = -\,\delta E_{\rm S}[n]/\delta n(\mathbf{r})$ (as the KS system is stationary when the potential is $v_{\rm S}(\mathbf{r})$).

This then defines a closed loop, once $E_{\rm HXC}[n]$ is known (or approximated), then $v_{\rm HXC}(\mathbf{r})$

can be found and an iterative cycle begins where the KS equation is solved to find a new density and the cycle repeats. At self-consistency $n(\mathbf{r})$ will be (or approximate) the molecular density and the total energy is given by Eq. 2.40. This is the Kohn-Sham approach[2].

Finally we note that the universal functional can be written in terms of the KS quantities, $F[n] = T_{\rm S}[n] + U[n] + E_{\rm XC}[n]$, where we separate $E_{\rm HXC}[n] = U[n] + E_{\rm XC}[n]$, as the Hartree energy $U[n]$ is known, but the exchange-correlation (XC) is not. The Hartree energy is defined as

$$U[n] = \frac{1}{2} \int d^3r \int d^3r' \; \frac{n(\mathbf{r})n(\mathbf{r}')}{|\mathbf{r} - \mathbf{r}'|} \tag{2.42}$$

leading to the KS potential being written as

$$v_{\rm S}(\mathbf{r}) = v(\mathbf{r}) + v_{\rm H}(\mathbf{r}) + v_{\rm XC}(\mathbf{r}) \tag{2.43}$$

where

$$v_{\rm H}(\mathbf{r}) = \frac{\delta U[n]}{\delta n(\mathbf{r})} = \int d^3r' \; \frac{n(\mathbf{r}')}{|\mathbf{r} - \mathbf{r}'|} \tag{2.44}$$

is the Hartree potential, and

$$v_{\rm XC}[n](\mathbf{r}) = \frac{\delta E_{\rm XC}[n]}{\delta n(\mathbf{r})} \tag{2.45}$$

is the XC potential.

With good approximations to $E_{\rm XC}[n]$, some of which are discussed next, this scheme has proven useful in many applications[5].

2.4.1 Exchange-Correlation functionals

The exchange-correlation functionals in common use can be loosely divided into two classes. Non-empirical functionals, largely developed by Perdew and co-workers[8], that start from the uniform and slowly-varying gases, and empirically-fitted functionals that are typically more accurate for systems close to the fit set[9, 10, 11]. The former apply more broadly and are more commonly used in physics, especially for bulk metals. The latter are more popular in chemistry, and are more accurate for specific systems and properties, such as transition-state barriers.

We start with the simplest approximation for the XC energy, namely the local density approximation (LDA)[2]. The LDA can be defined as follows, for a point $\mathbf{r}$ in space, with density $n(\mathbf{r})$ at the point, then the XC energy density as this point is that of a uniform electron gas with constant density $n_{\text{unif}} = n(\mathbf{r})$. For the exchange part, this can be found analytically:

$$E_{\text{X}}^{\text{LDA}}[n] = A_{\text{X}} \int d^3r \; n^{4/3}(\mathbf{r}) = \int d^3r \; \epsilon_{\text{X}}^{\text{LDA}}(n(\mathbf{r})) \tag{2.46}$$

where

$$A_{\text{X}} = -\frac{3}{4}\left[\frac{3}{\pi}\right]^{1/3} = -0.7386 \tag{2.47}$$

whereas for correlation, Monte-Carlo simulations were parameterized[] in order to write it as a density functional.

LDA works remarkably well given its simplicity, however it does not reach the levels of accuracy needed for chemical applications. Thus more complicated functionals have been developed and the widely used analogy is of a ladder of increasingly sophisticated density-functional approximations[12] leading up to heaven (chemical accuracy), but

at higher computational cost. We shall only concentrate on the next step up after LDA, the generalized gradient approximations.

If in LDA, the information given to the XC functional is just the density at a point, then to make a more accurate approximation, we could add information about how rapidly the density is varying at that point. Hence we make a semi-local approximation, i.e one which includes the gradient of the density. To do so, first we introduce the dimensionless measure of the gradient:

$$s(\mathbf{r}) = \frac{|\nabla n(\mathbf{r})|}{2k_{\mathrm{F}}(\mathbf{r})n(\mathbf{r})} \tag{2.48}$$

where $k_{\mathrm{F}}(\mathbf{r}) = (3\pi^2 n(\mathbf{r}))^{1/3}$ is the local Fermi wavevector. This is often written in terms of $x = |\nabla n|^2/n^{4/3}$, which is simply proportional to s. Assuming smoothness in s and no preferred spatial direction, we know any sensible approximation depends only on s^2. The gradient expansion is defined as the expansion of the energy as a functional of the density around the uniform limit. The leading correction for exchange is:

$$E_{\mathrm{X}}^{(2)}[n] = \mu \int d^3r\, s^2(\mathbf{r})\, \epsilon_{\mathrm{X}}^{\mathrm{LDA}}(n(\mathbf{r})), \tag{2.49}$$

where $\epsilon_{\mathrm{X}}^{\mathrm{LDA}}(n(\mathbf{r})) = A_{\mathrm{X}} n^{4/3}$ and μ is a constant. Alternatively, we may write:

$$E_{\mathrm{X}}^{(2)}[n] = -\beta \int d^3r\; n^{4/3}(r)\; x^2. \tag{2.50}$$

with

$$\beta = \frac{3}{16\pi}\left[\frac{1}{3\pi^2}\right]^{1/3} \mu. \tag{2.51}$$

In a very slowly-varying electron gas, the gradient is very small, and the exchange energy will be accurately given by $E_{\mathrm{X}}^{\mathrm{LDA}} + E_{\mathrm{X}}^{(2)}$. For such systems, the constant

$\mu = 10/81$[13], so that $\beta \approx 0.0024$.

The gradient expansion approximation (GEA) means applying this form to a finite system, using the value of μ from the slowly-varying gas. The GEA for exchange typically reduces the LDA error by about 50%. However it's counterpart for correlation worsens the LDA error, as its energy density is not even always negative. In many cases, GEA strongly overcorrects LDA leading to positive correlation energies and giving poor total energies[14].

A generalized gradient approximation (GGA) seeks to include the information contained in $s(\mathbf{r})$ while improving on the success of LDA. The B88 exchange functional was designed to reduce to the GEA form when s is small, but also recover the correct $-n(r)/2r$ decay of the exchange energy density for large r in atoms. Thus it interpolates between two known limits, and has the form:

$$\Delta E_{\mathrm{X}}^{\mathrm{B88}}[n] = -\beta^{\mathrm{B88}} \int d^3r \; n^{4/3}(r) \frac{x^2}{1 + 6x\beta^{\mathrm{B88}} \sinh^{-1}[2^{1/3}x]}, \tag{2.52}$$

where ΔE_{X} denotes the correction to LDA. Thus the B88 functional[9] contains one unknown parameter, β^{B88}. In 1988 Becke found this parameter by fitting to the Hartree-Fock exchange energies of the noble gases, finding a value of 0.0053. In fact, Becke notes that this value is consistent with the observation of a high-Z asymptote for β. In Ref. [15], Becke calculates what value of β in Eq. (2.50) is required in order to give the HF exchange energy for each atom in the first two rows of the periodic table along with the noble gas atoms. Thus, β is treated as a function of Z, and he observes that it converges for high-Z. Thanks to the previous section on asymptotic series, we can now understand why this convergence occurs. Although the B88 form reduces to that of the gradient expansion for small gradients, the value for β is about twice as large as that predicted from the slowly-varying gas.

Another common GGA for exchange is the Perdew-Burke-Ernzerhof (PBE) approximation[8], usually written in terms of an enhancement factor, $F_{\rm X}(s)$, to the LDA exchange energy density:

$$E_{\rm X}^{PBE}[n] = \int d^3r \; F_{\rm X}^{\rm PBE}(s) \; \epsilon_{\rm X}^{\rm LDA}[n] \tag{2.53}$$

where

$$F_{\rm X}^{PBE}(s) = 1 + \kappa - \frac{\kappa}{1 + \mu s^2/\kappa}, \tag{2.54}$$

and $\mu = 0.2195$ and $\kappa = 0.8040$. This form for the enhancement factor is chosen so that it reduces to LDA for $s = 0$ and again recovers the form of the gradient expansion for small s. For large s it becomes a constant determined by the parameter κ. Both κ and μ are determined via satisfaction of various exact conditions. The value of μ was chosen to preserve the good linear response of LDA for the uniform electron gas under a weak perturbation[16, 17], while κ is set by the Lieb-Oxford bound[18] on the exchange-correlation energy. (That condition is obviously violated by B88, while PBE does not accurately recover the X energy density in the tails of Coulombic systems).

2.4.2 Thomas-Fermi Theory

Before leaving DFT, we must discuss Thomas-Fermi (TF) theory[19, 20] which is now seen as the original DFT. It amounts to making an LDA-like approximation for the non-interacting kinetic energy functional, making no approximation to the XC energy, and minimizing the total energy functional directly. So we approximate the

universal functional as

$$F[n] \approx F^{\mathrm{TF}}[n] = T_{\mathrm{S}}^{\mathrm{LDA}}[n] + U[n] \tag{2.55}$$

where

$$T_{\mathrm{S}}^{\mathrm{LDA}}[n] = T_{\mathrm{S}}^{(0)}[n] = A_{\mathrm{S}} \int d^3r \; n^{5/3}(\mathbf{r}) \tag{2.56}$$

with $A_{\mathrm{S}} = (3/10)(3\pi^2)^{2/3}$. The total energy is written with this approximation and then minimized with respect to the density. This approach is often called pure-DFT or orbital-free-DFT to differentiate it from the standard KS DFT.

Although TF is not accurate for chemical applications, as we will see later, it has many interesting properties and in fact will serve as the major link between the semiclassical work of chapter 3 and DFT. In fact the link between WKB and Thomas-Fermi was studied as early as 1957[21].

Since we will work in 1d non-interacting systems, we will need the TF approximation in this case. The total energy is written as

$$E[n] = T_{\mathrm{S}}^{\mathrm{TF}}[n] + V_{\mathrm{ext}}[n] = \frac{\pi^2}{6} \int dx \; n^3(x) + \int dx \; n(x) \; v_{\mathrm{ext}}(x) \tag{2.57}$$

Finally note that just as for the GEA exchange energy, the TF kinetic energy density functional has gradient corrections, these will be introduced when they are needed in later chapters.

Chapter 3

Potential Functional Theory

The name potential functional theory (PFT) is not quite precise since one can say that everything is a functional of the potential. It is the potential that defines the system. As noted in the introduction, the exact solution of the Schrödinger equation would be called a potential functional. To clarify this ambiguity, PFT is an approximation that just uses the potential as input to directly yield a quantity without solving any Schrödinger equations. The WKB wavefunction of Eq. (2.27) is an example of a potential functional.

In this chapter, we will use semiclassical methods to analyze DFT and provide a derivation of potential functionals for the density and kinetic energy density that clearly show what DFT is missing. During the analysis of DFT, two topics emerged that required treatment in separate sections. Both use the scaling of the potential to shed new light on density functionals, the first of these finds new inequalities that the universal functional must obey and the second is a derivation (in the loosest sense) of the popular B88 exchange energy density functional. Finally we look at some of the implications for DFT that we can already see.

Semiclassical methods are standard in physics and in a tour-de-force, Schwinger[22] used semiclassical methods to rigorously derive the asymptotic expansion of the energies of neutral atoms for large Z. Now, in the pre-KS world of pure DFT, i.e., Thomas-Fermi and related theories, there is a long history of derivation of density functionals via semiclassical arguments, including the gradient expansion for both the kinetic[23] and exchange[13] energies, by considering an infinite slowly-varying electron gas. But its failure for finite systems led to these other approaches to XC functional construction.

To understand the essential difference between solids of moderate density variation and all finite systems, consider the cartoons of Fig. 3.1. Both prototypes can be treated semiclassically, i.e., via expansion in $\hbar$, which is equivalent to an expansion in gradients of the potential. For the valence electrons of a simple metal, the Fermi energy, E_F, is everywhere above the (pseudo)-potential, and periodic boundary conditions apply. This makes semiclassics simple, because there are no turning points, evanescent regions, or Coulomb cores. In finite systems (and typical insulators), E_F cuts the potential surface, leading to turning points and evanescent regions. Without a pseudopotential, there are also Coulomb cores, which require special treatment. The dominant term (in a sense specified below) in all cases is correctly given by the local density approximation, but in the latter case, there are important *quantum* corrections, which produce many features missing from semilocal density approximations, such as shell structure, self-interaction, etc.

Our semiclassical analysis applies to all systems, and explains the universality of local approximations (without mentioning the uniform gas). For slowly-varying densities, it is equivalent to the density-gradient expansion, but includes quantum corrections for other cases. These corrections explain why the gradient approximation had to be 'generalized' and why local and semilocal approximations miss essential features of

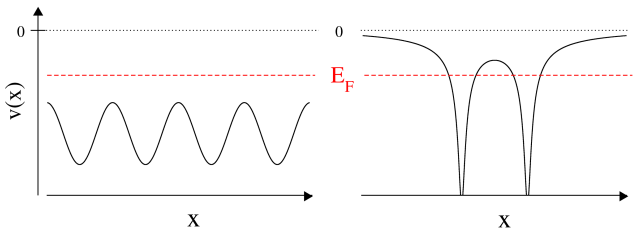

Figure 3.1: Cartoons of potential and Fermi energy in a simple metal (left) and molecule (right).

the kinetic energy. Insights based on our approach have already produced a revised version of PBE that is proving successful in many contexts[24]. Ultimately, the theory suggests that potential functionals[25] provide a more promising and systematic route to higher accuracy.

We illustrate this with a model in one dimension, and find much more accurate results by correcting this. We close with a discussion of the implications for modern DFT development.

3.1 What is missing in DFT?

We begin by discussing an asymptotic limit for all matter that corresponds to a semiclassical expansion, of which Schwinger's results are a specific example. The approach to the limit identifies the essential failure of the gradient expansion for finite systems. We (re)-introduce a potential scaling[26]:

$$v_{\rm ext}^{\zeta}(\mathbf{r}) = \zeta^{4/3}\, v_{\rm ext}(\zeta^{1/3}\mathbf{r}), \qquad N \to \zeta N, \tag{3.1}$$

where $v_{\rm ext}(\mathbf{r})$ is the one-body potential. For molecules with nuclear positions $\mathbf{R}_\alpha$ and charges Z_α, under this scaling, $Z_\alpha \to \zeta Z_\alpha$ and $\mathbf{R}_\alpha \to \zeta^{-1/3}\mathbf{R}_\alpha$. In an electric field,

$\mathcal{E} \to \zeta^{5/3}\mathcal{E}$. We say an approximation is large-N *asymptotically exact* to the p-th degree (AEp) if it recovers exactly the first p corrections for a given quantity under the potential scaling of Eq. (3.1). For neutral atoms, scaling ζ is the same as scaling Z, which is well-known:

$$E(\zeta) = -0.768745\,\zeta^{7/3} + \zeta^2/2 - 0.269900\,\zeta^{5/3} + ... \tag{3.2}$$

and is 'unreasonably accurate'[22], with less than 10% error even for H. An approximation that reproduces these three coefficients is AE2 and is likely to be very accurate. Lieb[26] showed that Thomas-Fermi theory becomes *exact* in the limit $\zeta \to \infty$ for *all* systems. However, TF theory recovers only the first term in Eq. (3.2), while Schwinger derived all three, but only for neutral atoms.

Because of this exactness for any system, as $\zeta \to \infty$,

$$n^\zeta(\mathbf{r}) \to \zeta^2 \left(n^{TF}(\zeta^{1/3}\mathbf{r}) + n^{QC}(\zeta, \mathbf{r})/\zeta^{1/3} + ... \right) \tag{3.3}$$

where n^{QC} becomes negligible compared to n^{TF} everywhere except in regions whose size is vanishing. So consider instead scaling the density rather than the potential, denoted by a subscript:

$$n_\zeta(\mathbf{r}) = \zeta^2\, n(\zeta^{1/3}\mathbf{r}). \tag{3.4}$$

This density-scaling is unusual, in that both the coordinate[27] and the particle number are scaled[28] (N to ζN). The universal functional is

$$F[n] = \min_{\Psi \to n} \langle \Psi |\, \hat{T} + \hat{V}_{\rm ee}\, | \Psi \rangle \tag{3.5}$$

where Ψ is any antisymmetric wavefunction with density $n(\mathbf{r})$ and $\hat{T}$ and $\hat{V}_{\rm ee}$ are the

kinetic and Coulomb repulsion operators, respectively. For large ζ, we find:

$$F[n_\zeta] = \zeta^{7/3}\, F^{TF}[n] + \zeta^{5/3}\, F^{WD}[n] + \zeta\, F_2[n] + ... \tag{3.6}$$

using the arguments of Ref. [29], i.e., that the gradients of the density become small almost everywhere under this scaling. Here $F^{TF}[n] = T_{\rm S}^{(0)}[n] + U[n]$, where $T_{\rm S}$ is the non-interacting KS kinetic energy, U the Hartree energy, and a superscript (j) denotes the j-th order contribution to the gradient expansion of a functional. The second term is $F^{WD}[n] = T_{\rm S}^{(2)} + E_{\rm X}^{(0)}$, i.e. the leading gradient correction to the kinetic energy, $T^W/9$, where $T^W = \int d^3r\, |\nabla n|^2/(8n)$ is the von Weizsäcker term[23], and the Dirac correction, i.e., the local approximation to exchange, while $F_2[n] = T_{\rm S}^{(4)} + E_{\rm X}^{(2)}$. Thus, scaling the density in this way justifies using the complete WD correction to TF theory (rather than just one or the other).

Next, we compare the expansion of Eq. (3.2) with that of Eq. (3.6). Since $T = -E$ for atoms, and $T \approx T_{\rm S}$ to the order we are working with, we see that ζ-scaling the density produces Eq. (3.6), which is the usual gradient expansion, but misses the ζ^2 term of Eq. (3.2). This quantum correction has long been recognized as missing from TF theory, but the gradient expansion misses it altogether. If TF theory is AE0, why is TFWD not AE1? The answer is that, for systems like those on the left of Fig 3.1, without turning points, edges, or Coulomb cores, there is no quantum correction, and the gradient expansion is the asymptotic expansion. For all others, there are quantum corrections to the energy, qualitatively changing its asymptotic expansion. Because $E_F \to \infty$ as $\zeta \to \infty$, these can be calculated with semiclassical techniques, just as Schwinger did for atoms.

To give an explicit example of these principles, we consider non-interacting spinless fermions in 1d in a potential $v(x)$ with infinite walls at $x = 0$ and L. For this case,

$v^\zeta(x) = \zeta^4\, v(\zeta x)$, and the analog of Eq. (3.6) is

$$T[n_\zeta] = \zeta^5\, T^{(0)}[n] + \zeta^3\, T^{(2)}[n] + \zeta\, T^{(4)}[n] + ... \tag{3.7}$$

where $T^{(0)} = \pi^2 \int dx\, n^3(x)/6$, $T^{(2)} = -T^W/3$, etc. [30]. Even a flat box ($v(x) = 0$) yields some insight. Then:

$$T^\zeta = \frac{\pi^2}{6L^2}\left(\zeta^5 N^3 + \zeta^4 \frac{3}{2} N^2 + \zeta^3 \frac{1}{2} N\right) \tag{3.8}$$

and the exact ground-state density is

$$n^\zeta(x) = \frac{k_F^\zeta}{\pi} - \frac{\sin(2k_F^\zeta x)}{2L\sin(\zeta \pi x/L)} \tag{3.9}$$

where $k_F^\zeta = \zeta\,\pi\,(\zeta\, N + 1/2)/L$. As $\zeta \to \infty$, $n \to \zeta^2 N/L$ and T is dominated by its leading term, agreeing with TF theory[26]. For $N = 1$, $T[n_\zeta] = \pi^2\,(5\zeta^5 - 2\zeta^3 + ...)/(12L^2)$, missing the quantum correction. The second term in Eq. (3.9) contains quantum oscillations and is of $O(\zeta)$, i.e., one order less, everywhere but at the edges (a region of size L/ζ), where it cancels the dominant term.

How can one calculate exactly the leading correction to the dominant term in $E[v^\zeta]$ for any system? As $\zeta \to \infty$, $v^\zeta(\mathbf{r})$ dominates over kinetic energy, and the system becomes semiclassical. In d dimensions, the diagonal Green's function for non-interacting particles satisfies:

$$g[v^\zeta](\hbar, \mathbf{r}, E) = \zeta^{1-4/d}\, g[v](\hbar/\zeta^{1/d}, \zeta^{1/d}\mathbf{r}, E/\zeta^{4/d}) \tag{3.10}$$

So as $\zeta \to \infty$, effectively $\hbar \to 0$. Furthermore, in 1d[31]:

$$g(x, E) = g^{\rm semi}(x, E)\left(1 + O\left(\frac{1}{E^{3/2}}\frac{dv}{dx}\right)\right) \tag{3.11}$$

where g^{semi} is approximated semiclassically. We can extract, e.g., the density from the Green's function, via Eq. (2.10), with C any contour in the complex energy E-plane that encloses all the eigenvalues $E_1, ..., E_N$ along the real axis. By choosing a vertical line along $\mathcal{E} = E_{\text{F}} + i\eta$, which is then closed by a large circle enclosing all the occupied poles, the smallest $|E|$ used is E_{F}, which is growing with ζ. The semiclassical approximation is *combined* with the best choice of contour to give a density error of $O(1/\zeta)$.

To illustrate how these quantum corrections can be found for both the density and the kinetic energy density, we use a 1d system with an arbitrary potential but with hard walls at $x = 0$ and $x = L$. Using the WKB approximation for this problem requires that $E_F > v(x)$ everywhere.

3.2 Semiclassical Density

If the WKB approximation, Eq (2.27), is used for $\psi_1(x)$ and $\psi_2(x)$ in Eq. (2.11) and then this Green's function inserted into Eq. (2.10), then an approximation to the density can be found. Also note that WKB yields the exact results for $v = 0$, but only once the boundary conditions are imposed. The WKB wavefunction satisfying the boundary conditions on the left is $\sin\theta(x)/\sqrt{k(x)}$, $\theta(x) = \int_0^x \mathrm{d}x'\ k(x')$ is the semiclassical phase, yielding

$$g^{\text{semi}}(x, E) = \frac{\cos\theta(L) - \cos\left[2\theta(x) - \theta(L)\right]}{k(x)\sin\theta(L)}. \tag{3.12}$$

where for brevity we drop the E argument of $\theta(x)$, $\theta(L)$, and $k(x)$. The first term yields the TF result using $\cot[\theta(L)] \to -i$ as the dominate piece when we shift off the real axis and perform the contour integral as shown in Fig. 3.2

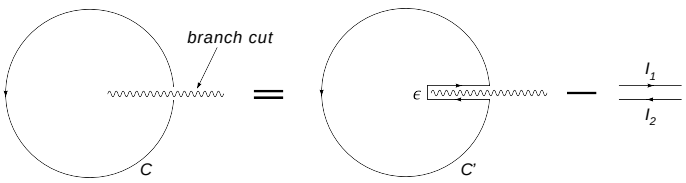

Figure 3.2: The contour in the complex energy plane is split into two parts due to the branch cut along the real axis, starting at $E = v(x)$.

Thus we find that the dominate correction is

$$n^{\mathrm{TF}}(x) = \frac{k_F(x)}{\pi} \tag{3.13}$$

where the subscript F implies evaluation at E_F. This then leaves the quantum correction to TF as

$$n^{\mathrm{QC}}(x) = -\frac{1}{4\pi} \oint_C \frac{dE}{k(x)} \, \frac{e^{2i\theta(x)} + e^{-2i(\theta(x)-\theta(L))}}{e^{2i\theta(L)} - 1} \tag{3.14}$$

The semiclassical quantization condition is $\theta(L)/\pi$ an integer, so $\theta_F(L) = \pi(N + \delta), 0 \leq \delta \leq 1$. The most convenient choice is $\delta = 1/2$. As $N \to \infty$, $E_{\mathrm{F}} >> \eta$ for the dominant contributions to the integral, so we expand all quantities to first order in η. This is the same as the ℓ contour used in Ref. [31]. Substituting $u = T_{\mathrm{F}}\eta$ and $y = \tau_{\mathrm{F}}(x)/T_{\mathrm{F}}$,

$$n^{\mathrm{QC}}(x) = -\frac{\Im\{e^{2i\theta_{\mathrm{F}}(x)}\}}{2\pi T_{\mathrm{F}} k_{\mathrm{F}}(x)} \int_0^\infty \mathrm{d}u \frac{e^{-yu} + e^{-(1-y)u}}{e^{-u} + 1}, \tag{3.15}$$

with $\tau_{\mathrm{F}}(x) = \int_0^x \mathrm{d}x'/k_{\mathrm{F}}(x')$ the classical time for a particle at E_{F} to travel from 0 to x, $T_{\mathrm{F}} = \tau_{\mathrm{F}}(L)$, and finally

$$n^{\mathrm{semi}}(x) = \frac{k_{\mathrm{F}}(x)}{\pi} - \frac{\sin 2\theta_{\mathrm{F}}(x)}{2T_{\mathrm{F}}\, k_{\mathrm{F}}(x) \sin\alpha(x)}, \tag{3.16}$$

where $\alpha(x) = \pi\tau_{\mathrm{F}}(x)/T_{\mathrm{F}}$.

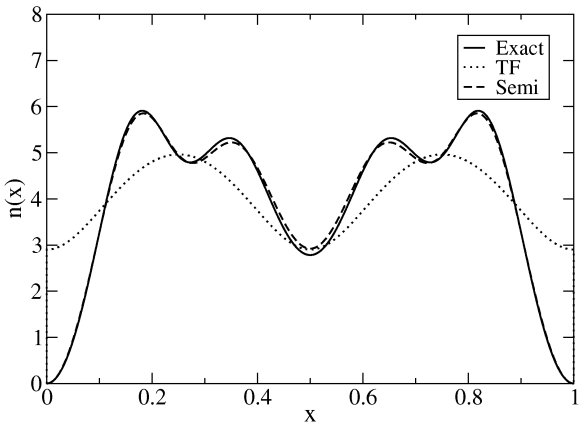

Figure 3.3: Densities for $v(x) = -80\sin^2(2\pi x)$ for $N = 4$.

We plot results for $v(x) = -80\sin^2(2\pi x)$, a well with two deep valleys. The four lowest single particle energies are $-46.32, -42.50, 10.18, 37.25$, so that the lower two have turning points. In Fig. 3.3, we show the density, both exact and approximate, for $N = 4$ particles. The density is not automatically normalized, but its error is less than 0.2%.

Evaluating $T_{\rm S}^{(0)}$ tests the accuracy of a density: The exact value is 153.0, it is 115.5 in self-consistent TF, 114.6 in non-self-consistent TFW, and 151.4 for $n^{\rm semi}$.

Although the lower two eigenstates will have turning points where $v_{\rm ext}(a) = \epsilon_j$, the Fermi energy does not, allowing us to use Eq. (3.16). We do not deal with turning points in this work, prefering to work with this type of system as it is less complicated and easily to see the quantum corrections. We use the semiclassical approximation of Airy functions to deal with this case, but this is work as yet unpublished.

The exact solution was found numerically by solving the solving the Schrödinger equation on a real space grid using a finite-difference method for the derivative in the kinetic energy. The Fermi energies are found using the Newton method described in the appendix B.

3.3 Semiclassic Kinetic Energy Density

The kinetic energy density (KED) may be defined in two ways:

$$\tau^1(x) = -\frac{1}{2}\sum_{j=1}^{N} \psi_j^*(x)\partial_x^2\psi_j(x) \tag{3.17}$$

and

$$\tau^2(x) = +\frac{1}{2}\sum_{j=1}^{N} |\partial_x\psi_j(x)|^2 \tag{3.18}$$

Both integrate to the same quantity $T_{\rm S}$, the total kinetic energy,

$$T_{\rm S} = \int \tau^1(x)dx = \int \tau^2(x)dx \tag{3.19}$$

as can be seen by an integration by parts with the requirement that $\psi_j(x) \to 0$ as $x \to \pm\infty$. This will not be true for systems with periodic boundary conditions. We will use the definition:

$$\tau(x) = \sum_{j=1}^{N}(\epsilon_j - v(x))|\psi_j(x)|^2 \tag{3.20}$$

This definition will yield the same KED as $\tau^1(x)$, as can be seen by inserting the definition of ϵ_j from Eq. (2.6) into Eq. (3.20). In the 1DSE code written, this is the definition used. We may use a similar definition to write $\tau(x)$ in terms of the Green's function

$$\tau(x) = \frac{1}{2\pi i}\oint_C dE\ k^2(x)G(x;E) \tag{3.21}$$

We use the same Green's function as for the density, Eq. (3.12), and insert into Eq.

(3.21).

$$\tau(x) = \frac{1}{2\pi i} \oint_C dE\ k(x)\ \frac{\cos[\theta(L)] - \cos[2\theta(x) - \theta(L)]}{\sin[\theta(L)]} \tag{3.22}$$

Picking out the dominate piece of Eq. (3.22) when E has a small imaginary part and either the particle number or the box size is large gives the Thomas-Fermi (TF) kinetic energy density

$$\tau^{\rm TF}(x) = \frac{k_{\rm F}^3(x)}{6\pi} \tag{3.23}$$

If the Thomas-Fermi contribution is subtracted off, then the kinetic energy density will be

$$\tau(x) = \tau^{\rm TF}(x) + \tau^{\rm OSC}(x) \tag{3.24}$$

where

$$\tau^{\rm OSC}(x) = \frac{1}{2\pi i} \oint_C dE\ k(x)\ \frac{\exp[i\theta(L)] - \cos[2\theta(x) - \theta(L)]}{\sin[\theta(L)]} \tag{3.25}$$

We choose the same contour as for the quantum corrections to the density, along ℓ where $E = \epsilon_{\rm F} + i\xi$ and ξ goes from $0 \to \infty$. We also choose $\epsilon_{\rm F}$ to be always larger than ξ and thus we can expand quantities in ξ. This can be done as we know from Ref. [31] that the integrand falls off as $1/E^2$ in the complex E plane. The final expression

can be written as:

$$\begin{aligned}\tau^{\rm OSC}(x) &= k_{\rm F}^2(x)n^{\rm OSC}(x)\left(1+\beta(x)\gamma(x)\right)/2 \\ &- \frac{k_{\rm F}(x)\beta(x)}{4T_{\rm F}}\left(\frac{1}{6}+\cot[\alpha(x)]\frac{\cos 2[\theta_{1F}(x)]}{\sin[\alpha(x)]}\right)\end{aligned} \tag{3.26}$$

where $\beta(x)=\pi[T_{\rm F}^{(2)}/T_{\rm F}+k_{\rm F}^{-2}(x)]/(2T_{\rm F})$, $\gamma(x)=\pi(1/2-\csc^2[\alpha(x)])/(2k_{\rm F}^2(x)T_{\rm F})$,$T_{\rm F}=T(\epsilon_{\rm F})$ and $T_F^{(2)}=\int_0^L dx'/p_F^3(x')$.

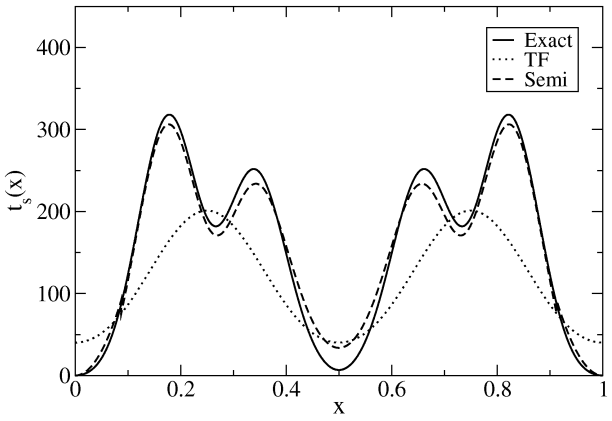

Figure 3.4: Kinetic energy densities of Fig. 3.3.

We plot results for the same potential as for Fig. 3.3, $v(x)=-80\sin^2(2\pi x)$. In fact, $t_{\rm S}^{\rm semi}$ is ill-behaved right at the end points, so we model its approach to the boundaries with a simple parabola for $x<0.0875$, with constant chosen to match the logarithmic derivative at that point. The resulting integrated $T_{\rm S}$ is 156.2, compared to the exact result 157.2.

We emphasize that the correct semiclassical treatment has reduced the error in self-consistent TF theory by a factor of 40. Thus the semiclassical approach is far more powerful and systematic than the usual gradient expansion. How then do density

functionals achieve the accuracy needed for chemical and materials applications? The answer already appears for the flat box. Inserting the *exact* density in $T^{(0)}$ yields $\frac{\pi^2}{6L^2}(\zeta^5 N^3 + \zeta^4 \frac{9}{8} N^2 + \zeta^3 \frac{3}{8} N)$, i.e. reasonably accurate quantum corrections, because most of the contribution comes from regions of not-too-rapidly varying density. In the double-well potential, $T_{\rm S}^{(0)}$ on the exact density is only 4 times worse than our semiclassical approximation. Thus semilocal functionals, applied to the highly accurate densities from the KS scheme, contain typically good approximations to the quantum corrections in the energy. In fact, for the flat box, the leading gradient correction *worsens* the energy. If we alter the coefficient of T^W from $-1/3$ to $+0.424$, the corresponding 'generalized' gradient expansion is AE1, and far more accurate for particles in boxes.

3.4 Including gradient terms

We can include terms of higher order in $\hbar$ in the WKB wavefunction to find gradient corrections to the semiclassical kinetic energy formula, Eq. (3.26). Careful analysis of this formula shows that it includes terms of order $\hbar^2$. As we shall see, the next order gradient correction to Thomas-Fermi is of order $\hbar$, hence to be a complete semiclassical description, one must include these terms. Below I shall simply demonstrate that using the WKB wavefunction with higher order terms and the Green's function methods developed above, one can recover the known gradient correction to TF[30]. However, since quantum correction terms can also be found by including these terms, we can go further than these simple corrections. This is an obvious candidate for future work and may shed light on the generalized gradient corrections of DFT.

Recall that for higher order WKB, the wavefunction is given by

$$\phi(x) = \frac{c}{\sqrt{Q(x)}} \sin[\frac{1}{\hbar}\int^x dx' Q(x')] \tag{3.27}$$

where to next order

$$Q(x) = k(x) + \hbar^2 Q^{(2)}(x) \tag{3.28}$$

and

$$Q^{(2)}(x) = +\frac{v''(x)}{4k^3(x)} + \frac{5[v'(x)]^2}{8k^5(x)} \tag{3.29}$$

If we now construct the Green's function

$$G(x,x';E) = -\frac{2\sin\left[\gamma_1(x;E)\right]\sin\left[\gamma_2(x;E)\right]}{\hbar\sqrt{Q(x;E)Q(x';E)}\sin\left[\Gamma(E)\right]} \tag{3.30}$$

where

$$\begin{aligned}
\gamma_1(x;E) &= \gamma(x;E) = \frac{1}{\hbar}\int_0^x Q(x'';E)dx'' && (3.31)\\
\gamma_2(x;E) &= \frac{1}{\hbar}\int_{x'}^L Q(x'';E)dx'' && (3.32)\\
\Gamma(E) &= \frac{1}{\hbar}\int_0^L Q(x'';E)dx'' && (3.33)
\end{aligned}$$

If we first calculate the TF like term, $\tau_1(x)$, TF in the sense that this gives TF to first order and we calculate the contour integral in the same manner. As in the previous case, we shift off the real axis and follow the contour of Fig. 3.2, then

$$\tau_1(x) = -\frac{1}{4\pi\hbar}\oint_{E_F} dE\ \frac{[k(x;E)]^2}{Q(x;E)} \tag{3.34}$$

integrates to

$$\tau_1(x) = \frac{k_F^3}{6\pi\hbar} + \hbar\left[\frac{v''}{8\pi k_F} + \frac{5v'^2}{48\pi k_F^3}\right] \tag{3.35}$$

using

$$\frac{1}{Q} = \frac{1}{k} - \hbar^2\left(\frac{v''}{4k^5} + \frac{5v'^2}{8k^7}\right) + ... \tag{3.36}$$

This is exactly the gradient correction to Thomas-Fermi as calculated in Ref. [30].

3.5 Potential Scaling

Density scaling has been a particularly useful tool for the analysis and development of DFT. A singular example is uniform coordinate scaling[27], where the coordinates of a given density are linearly scaled, but normalization is preserved. This has led to fundamental exact conditions on the exchange-correlation (XC) energy functional[27, 32, 33, 34]. For example, the form of the local approximation to the exchange energy can be deduced from this scaling. The adiabatic-connection formulation[35, 36, 37, 38], much studied and used in DFT development, is essentially an integral over the uniform coordinate scaling parameter[27, 39, 40]. Here, the electron-electron interaction is scaled by a constant while the density is kept fixed, linking the non-interacting Kohn-Sham and the fully interacting systems, and leads to many more conditions. For example, the adiabatic connection formula is behind rationalizing the hybrid approach[41, 42, 43, 44].

Recently, a different form of density scaling was used in the development of the PBEsol functional[45]. Here, both the coordinate and the particle number are scaled, leading to new insights into the XC functional. We refer to this as charge-neutral scaling[29],

as it is equivalent to simultaneously changing the charges on atoms and the number of electrons, so as to keep overall neutrality.

In this section, we extend the use of density scaling as a tool in DFT. Most importantly we introduce the concept that any form of density scaling defines a related form of potential scaling. This leads to more exact conditions on the various DFT quantities as functionals of densities of different particle number. Yang and others[25] have emphasized the duality of the potential with the density, but have not related scaling of one to the other.

Potential Scaling

Consider a density $n(\mathbf{r})$ that is the ground-state density of some interacting problem with potential $v_{\text{ext}}(\mathbf{r})$. Now, introduce some positive parameter, $0 < \gamma < \infty$, which produces a family of densities, $n_\gamma(\mathbf{r})$, with γ defined so that $\gamma \to \infty$ corresponds to the high-density limit.

A simple example is the uniform coordinate scaling of Levy and Perdew[27]:

$$n_\gamma(\mathbf{r}) = \gamma^3 n(\gamma \mathbf{r}), \qquad 0 < \gamma < \infty, \tag{3.37}$$

where the prefactor was chosen to keep the density normalizd. For example, under uniform coordinate scaling with $\gamma > 1$, the density of He is squeezed into a smaller volume, and looks like a distorted version of a two-electron ion[46]. This scaling has become a mainstay of DFT and leads to many important results. Most importantly, when particles interact, the coordinate-scaled wavefunction is not the ground-state wavefunction of the scaled density. Considering such a wavefunction as a trial state in the Rayleigh-Ritz principle yields useful inequalities for the various

density functionals[27]:

$$T[n_\gamma] \leq \gamma^2\, T[n], \qquad \gamma \geq 1, \tag{3.38}$$

$$V_{\rm ee}[n_\gamma] \geq \gamma\, V_{\rm ee}[n], \qquad \gamma \geq 1, \tag{3.39}$$

and a similar condition applies for the correlation energy $E[n]$ itself.

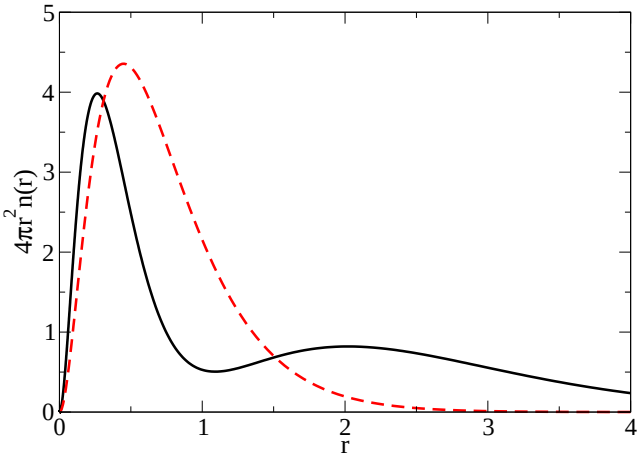

Figure 3.5: The exact radial densities of Beryllium (solid line)[47], and of the CN scaled (with $\zeta = 2$) Helium (dashed line)[48].

A second example that we focus on here is what we call charge-neutral (CN) scaling, in which

$$n_\zeta(\mathbf{r}) = \zeta^2 n(\zeta^{1/3}\mathbf{r}), \qquad 0 < \zeta < \infty \tag{3.40}$$

and so $N_\zeta = \zeta N$. We use ζ as the scaling parameter to distinguish from coordinate scaling. This choice both scales the coordinate *and* changes the particle number. For Coulomb-interacting matter, this ensures neutrality as a function of ζ. For example,

for single atoms, it simply implies $Z_\zeta = \zeta Z$ and the atom remains neutral. Lieb and Simon[49] showed that Thomas-Fermi (TF) theory becomes exact for neutral atoms as $\zeta \to \infty$, and Lieb[26] later generalized the proof to all Coulomb-interacting matter. In Fig 1, we illustrate this scaling on the He atom density.

In both coordinate and CN scaling, as the scaling parameter is taken to ∞, the solution simplifies. Under uniform coordinate scaling to the high-density limit, the system becomes effectively non-interacting. Under CN scaling to the high-density limit, Thomas-Fermi theory becomes relatively exact. In either case, we can ask how the potential changes when the density is scaled. We define this as the potential scaling conjugate to the given density scaling, but consider it for all values of the scaling parameter, not just in the high-density limit.

Under coordinate scaling, in the large γ limit,

$$v^\gamma(\mathbf{r}) = \gamma^2 v(\gamma \mathbf{r}). \tag{3.41}$$

We therefore define our potential scaling by this equation, applied for all γ. We use a superscript to indicate that the potential has been scaled, not the density. This is simply how the external potential would change when the density is scaled, if the particles were non-interacting particles. For example, for a neutral atom, this changes the nuclear charge by γ, keeping the particle number fixed. As $\gamma \to \infty$, the repulsion between electrons becomes negligible relative to the nuclear attraction, and the density becomes that of the non-interacting limit, scaled by γ.

Similarly, under CN scaling with $\zeta \to \infty$, the TF equations become relatively exact[50], and

$$v^\zeta(\mathbf{r}) = \zeta^{4/3} v(\zeta^{1/3}\mathbf{r}), \qquad N_\zeta = \zeta N. \tag{3.42}$$

Again, the conjugate potential scaling is defined by this, applied to all values of ζ. Analogously, if self-consistent TF theory were exact, this is how the potential would scale for any ζ as the density is scaled.

Although chosen to match the corresponding density scaling in the high-density or high-potential limit, these potential scalings can be applied for any values of their scaling parameter. Since scaling the potential is much more common in quantum problems than scaling the density, often solutions are known or can be accurately calculated for different scalings of the potential, but not of the density. In this paper, we find relations and inequalities between such solutions that complement the ground-breaking results of the previous generation[27].

Uniform coordinate scaling

In the old work[27], Levy and Perdew compared two different wavefunctions with the same density, whereas we compare two different wavefunctions in the same potential. To do this, begin from a given potential $v_{\rm ext}(\mathbf{r})$ with ground-state density $n(\mathbf{r})$. Define $n^\gamma(\mathbf{r})$ as the ground-state density of $v^\gamma_{\rm ext}(\mathbf{r})$, given by Eq. (3.41). Then $n^\gamma_{1/\gamma}(\mathbf{r})$ is a useful trial density for the original problem. It is found by first scaling the potential, solving the problem, and then scaling backwards to the original problem. (In Fig. 1, the dashed line corresponds $n^\zeta(\mathbf{r})$ for the He density, with $\zeta = 2$.) This is exactly what was done (but with an approximate scale factor) in Ref. [46].

If $n^\gamma_{1/\gamma}(\mathbf{r})$ is used as trial density for $v_{\rm ext}(\mathbf{r})$, the variational principle states that

$$F[n^\gamma_{1/\gamma}] + \gamma^{-2} V^\gamma_{\rm ext}[n^\gamma] \geq F[n] + \gamma^{-2} V^\gamma_{\rm ext}[n_\gamma], \tag{3.43}$$

which may be rearranged as

$$F[n^\gamma_{1/\gamma}] - F[n] \geq \gamma^{-2}(V^\gamma_{\rm ext}[n_\gamma] - V^\gamma_{\rm ext}[n^\gamma]). \tag{3.44}$$

Conversely, $n_\gamma(\mathbf{r})$ may be used as a trial density for $v^\gamma_{\rm ext}(\mathbf{r})$, yielding

$$\begin{aligned} E_{v^\gamma_{\rm ext}}[n_\gamma] &= F[n_\gamma] + V^\gamma_{\rm ext}[n_\gamma] \\ &\geq F[n^\gamma] + V^\gamma_{\rm ext}[n^\gamma], \end{aligned} \tag{3.45}$$

which can also be rearranged as

$$F[n^\gamma] - F[n_\gamma] \leq V^\gamma_{\rm ext}[n_\gamma] - V^\gamma_{\rm ext}[n^\gamma]. \tag{3.46}$$

Combining the two inequalities yields a constraint on the universal functional $F[n]$:

$$F[n^\gamma_{1/\gamma}] - \frac{F[n^\gamma]}{\gamma^2} \geq F[n] - \frac{F[n_\gamma]}{\gamma^2}, \tag{3.47}$$

which may be written in a concise form, with $\lambda = 1/\gamma$,

$$\Delta F^\lambda[n^{1/\lambda}_\lambda] \geq \Delta F^\lambda[n], \tag{3.48}$$

where

$$\Delta F^\lambda[n] = F[n] - \lambda^2 F[n_{1/\lambda}]. \tag{3.49}$$

Now, $F[n]$ is typically dominated by the kinetic energy contribution, but this can be removed, because $T_{\rm S}[n_\gamma] = \gamma^2\, T_{\rm S}[n]$. Thus

$$\Delta E^\lambda_{\rm HXC}[n^{1/\lambda}_\lambda] \geq \Delta E^\lambda_{\rm HXC}[n], \tag{3.50}$$

where $E_{\rm HXC} = U + E_{\rm XC}$. This tells us that if we begin from, e.g., the lowest value of Z that binds a given N electrons, then $\Delta E^\lambda_{\rm HXC}[n^{1/\lambda}_\lambda]$ is an increasing function of λ.

Simple results can be extracted from this very general formula by taking γ to be very large. This makes $n^\gamma(\mathbf{r})$ an essentially non-interacting density, because the external potential dominates. Thus

$$n_\lambda^{1/\lambda}(\mathbf{r}) \to n_{\rm NI}(\mathbf{r}), \qquad \lambda \to 0, \tag{3.51}$$

where $n_{\rm NI}(\mathbf{r})$ is the density of the system with only an infinitesimal electron-electron repulsion. But $\Delta E^\lambda_{\rm HXC}[n]$ also simplifies as $\lambda \to 0$, because all terms scale less than quadratically. Thus

$$\Delta E^\lambda_{\rm HXC}[n] \to E_{\rm HXC}[n], \qquad \lambda \to 0, \tag{3.52}$$

yielding the universal result that

$$E_{\rm HXC}[n_{\rm NI}] \geq E_{\rm HXC}[n], \tag{3.53}$$

applying to all potentials. For $\gamma < 1$, Eq. (3.48) is less useful, as most systems of interest lose an electron when the external potential becomes too small. To further simplify Eq. (3.50), we note that both the Hartree and exchange energies scale linearly with γ, i.e.,

$$E_{\rm HX}[n_\gamma] = \gamma\, E_{\rm HX}[n], \tag{3.54}$$

so that

$$\Delta E^\lambda_{\rm HX}[n] = (1-\lambda)\, E_{\rm HX}[n]. \tag{3.55}$$

Table 3.1: The Hartree energies, U, for the helium iso-electronic series as calculated with the oep exact-exchange method as implemented in the OPMKS code[51]. We also demonstrate how, for two values of atomic number Z', the inequalities of Eq. (3.59) with $\gamma = Z'/Z$, are satisfied. Note that if $\gamma < 1$, the inequality is reversed. The values for bordering values of Z bracket the value of U at atomic number Z and these bounds become tighter as Z' increases.

Z	U	Z'=4	Z'=20
1	0.790970	3.163880	15.819400
2	2.051538	4.103076	20.515380
3	3.303373	4.404497	22.022487
4	4.554137	4.554137	22.770685
6	7.054819	4.703213	23.516063
10	12.055315	4.822126	24.110630
20	24.555661	4.911132	24.555661

Inserted into Eq. (3.50), we find

$$E_{\rm HX}[n^\gamma_\lambda] + \Delta' E^\lambda_{\rm c}[n^\gamma_\lambda] \geq E_{\rm HX}[n] + \Delta' E^\lambda_{\rm c}[n], \tag{3.56}$$

where

$$\Delta' E^\lambda_{\rm c}[n] = \Delta E^\lambda_{\rm c}[n]/(1-\lambda). \tag{3.57}$$

The simplest way to test this result is by doing a Kohn-Sham calculation without any correlation (such as oep exact exchange). Then the correlation contributions vanish on both sides of Eq. (3.56), and so

$$E_{\rm HX}[n] \leq E_{\rm HX}[n^\gamma]/\gamma \leq E_{\rm HX}[n_{\rm NI}] \tag{3.58}$$

This simplifies even further for the special case of two electrons in a spin singlet, where $E_{\rm X}[n] = -U[n]/2$, so the inequality becomes a bound on the Hartree energy

Table 3.2: Hartree-exchange energies for the beryllium iso-electronic series. Values were also calculated with the OPMKS code with oep exact-exchange. Also shown are two examples of the inequalities of Eq. (3.58), again using $\gamma = Z'/Z$. Although the quantities are more complicate that those in Table 3.1, the overall trend is the same.

Ion	Z	E_{HX}	Z'=10	Z'=16
Be	4	4.489776	11.224440	17.959104
B^{+}	5	6.119120	12.238240	19.581184
O^{4+}	8	10.893545	13.616931	21.787090
Ne^{6+}	10	14.051482	14.051482	22.482371
S^{12+}	16	23.498356	14.686473	23.498356
Ca^{16+}	20	29.788628	14.894314	23.830902

alone:

$$U[n] \leq U[n^{\gamma}]/\gamma \leq U[n_{\text{NI}}] \tag{3.59}$$

In Table 3.1, we analyze the above inequality, Eq. (3.59), while in Fig 3.6, we plot $U[n^{\gamma}]/\gamma$ as a function of γ for exact-exchange calculations of the two-electron ion series, beginning with H^{-}. Indeed, the function increases toward the Bohr atom limit of 5/4, found by inserting a doubly-occupied 1s Hydrogen atom orbital into the Hartree energy.

To test the exchange contribution in a non-trivial way, i.e., Eq. (3.56), we repeated the calculations for the four-electron ion series, this time beginning from Be. Again the inequality is satisfied, and the limiting value is found by evaluating the Hartree and exchange energies of doubly-occupied 1s and 2s Hydrogenic orbitals, as calculated in Appendix A. These values are reported in Table 3.2 and plotted in Fig 3.7.

Lastly, we can even include extremely accurate estimates of the correlation contributions for the two-electron series. We work from the data in Table I of Ref. [52]. Since the two-electron ions are generally weakly correlated, one can approximate the scaling of their correlation energies with a Taylor-series around the high-density limit:

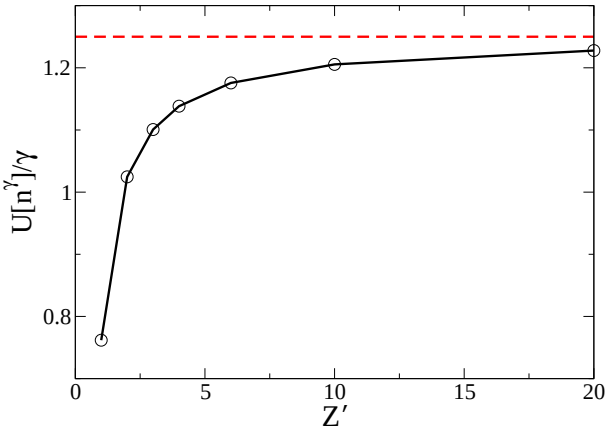

Figure 3.6: Using the Hartree energies from Table 3.1, Eq. (3.59) is illustrated for $\gamma = Z'/Z$ and $Z = 1$. The trend is identical to that seen in Table 3.1, however it is clear that the value is approaching it's asymptote, 5/4. This is the Hartree energy for density consisting of the doubly occupied hydrogen 1s orbital.

$$E_{\rm C}[n] = E_{\rm C}^{(0)}[n] + \lambda\, E_{\rm C}^{(1)}[n] \tag{3.60}$$

where $E_{\rm C}^{(p)}[n]$ are scale-invariant functionals. Since $T_{\rm C} = -E_{\rm C} + \partial E_{\rm C}[n\gamma]/\partial\gamma(\gamma = 1)$[27], and $T_{\rm C}$ is reported in their table, one can solve for these two coefficients. This yields a value of -47.6 mH for $E_{\rm C}^{(0)}$ for He, in excellent agreement with the value of 47.9 estimated in Ref. [46], and predicts a value of -56.1 mH for H^-. Using this approximate scaling, we can insert all terms into Eq. (3.50) explicitly and find their behavior. The numerical corrections to our previous results are negligible.

Charge-neutral Scaling

In this section, we repeat all the logic of the previous section, but apply it now to CN scaling. After repeating similar steps (given in Appendix C), we arrive at the general

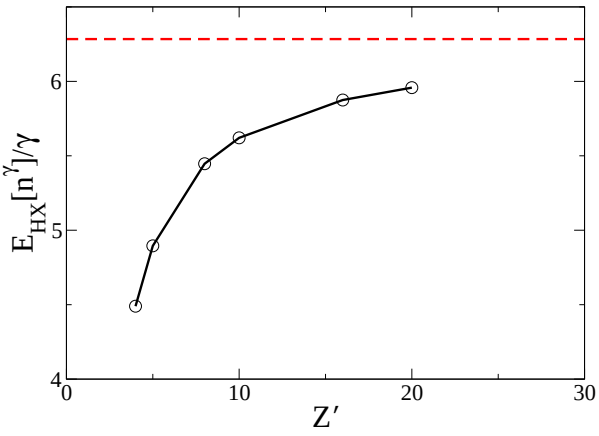

Figure 3.7: The Hartree-exchange energies reported in Table 3.2 are used to illustrate the inequalities of Eq. (3.58) with $\gamma = Z'/Z$ and $Z = 4$. Compared to Fig. 3.6, the value of $E_{\rm HX}[n^\gamma]/\gamma$ is not as fully converged to its asymptote, however the maximum value of γ is 4 times smaller. The asymptotic value for this case is $586373/93312 = 6.284$, which is found by doubly occupying both 1s and 2s hydrogenic orbitals with $Z = 4$ and calculating Hartree and exchange energies.

result:

$$\Delta F^\alpha[n_\alpha^{1/\alpha}] \geq \Delta F^\alpha[n] \ , \tag{3.61}$$

where

$$\Delta F^\alpha[n] = F[n] - \alpha^{7/3} F[n_{1/\alpha}] \ , \tag{3.62}$$

and $\alpha = 1/\zeta$. Just as we did for coordinate scaling, we can refine our inequality substantially. By construction, $\Delta F^\alpha[n] = 0$ for $F^{\rm TF}[n]$, so we define the useful functional:

$$F^{NT}[n] = F[n] - F^{\rm TF}[n] \tag{3.63}$$

as the *Non*-Thomas-Fermi contribution to $F[n]$. Our inequality then reads:

$$\Delta F^{NT\alpha}[n_\alpha^{1/\alpha}] \geq \Delta F^{NT\alpha}[n] \ , \tag{3.64}$$

where

$$\Delta F^{NT\alpha}[n] = F^{NT}[n] - \alpha^{7/3} F^{NT}[n_{1/\alpha}] \ . \tag{3.65}$$

We find an interesting result in the limit $\alpha \to 0$, if we make the reasonable assumption that all non-Thomas-Fermi contributions scale less strongly than $\zeta^{7/3}$:

$$F^{NT}[n^{\mathrm{TF}}] \geq F^{NT}[n] \ , \tag{3.66}$$

as TF becomes relatively exact in the high ζ. This inequality is fiendishly hard to test, even in the large ζ limit. Consider, e.g., the He atom. The corresponding TF density is well-known[53] but we would have to evaluate the exact interacting functional on it to find the non-TF contribution. All the above results also apply directly to non-interacting electrons in a potential, such as the Bohr atom[54], with F replaced by T_{s}, and the TF contributions calculated with no Hartree term. But the same difficulties remain.

There is one case where we know enough already to test. For the hydrogen atom (or any one-electron system), $F = T$ only, and is given by the von Weizacker functional. The TF density (with or without interaction) is well-known and singular at the origin, making the von Weizacker energy diverge. Thus, the formula is satisfied, but not very informative.

Lastly, we consider Thomas-Fermi-Dirac-Weizsäker theory[23] (TFDW). Here we add

to TF the local exchange

$$E_{\rm X}^{(0)}[n] = A_{\rm X} \int d^3r \; n^{4/3}(\mathbf{r}), \tag{3.67}$$

where $A_{\rm X} = -(3/4)(3/\pi)^{1/3}$, and the next order gradient correction to the kinetic energy,

$$T_{\rm S}^{(2)}[n] = \frac{1}{72} \int d^3r \; \frac{|\nabla n(\mathbf{r})|^2}{n(\mathbf{r})}. \tag{3.68}$$

Both these terms scale the same way under CN density scaling, i.e.,

$$F^{(2)}[n_\zeta] = T^{(2)}[n_\zeta] + E_{\rm X}^{(0)}[n_\zeta] = \zeta^{5/3}(T^{(2)}[n] + E_{\rm X}^{(0)}[n]). \tag{3.69}$$

Then can write the inequality as

$$F^{(2)}[n^\zeta] \geq \zeta^{5/3} F^{(2)}[n], \tag{3.70}$$

where $n(\mathbf{r})$ has been evaluated self-consistently within TFDW and $\zeta \geq 1$. Thus

$$F^{(2)}[n^{\rm TF}] \geq F^{(2)}[n^\zeta]/\zeta^{5/3} \geq F^{(2)}[n], \tag{3.71}$$

where $n^{\rm TF}(\mathbf{r})$ is the Thomas-Fermi solution for the same potential as for $n(\mathbf{r})$.

Conclusion

Potential scaling, conjugate to a given density scaling, promises to be a useful tool in density functional theory. It leads to many exact conditions that can be used in functional construction. We have applied it to two distinct types of scaling: uniform coordinate scaling and charge neutral scaling. In both cases, we have found several interesting bounds. Uniform coordinate scaling was useful for analyzing Kohn-

Sham DFT, leading to inequalities involving the only unknown in DFT, the exchange-correlation functional. The limit of this inequality involves evaluating the Hartree-exchange-correlation energy of the density of non-interacting fermions in the external potential. This connection between the interacting and non-interacting systems resonates with standard approaches in many-body perturbation theory. We illustrate the bounds on the Hartree-exchange energy this inequality provides by performing OEP exact exchange calculations on helium and beryllium, showing the approach to their asymptote. On the other hand, charge-neutral scaling provides inequalities involving Thomas-Fermi quantities. The Thomas-Fermi approximation becomes relatively exact for all electronic systems[49, 26] and these relations link the corrections to Thomas-Fermi with the true system, including those of TFDW theory. However evaluating the TF density within these theories often leads to divergences[55, 56]. In the derivation of these inequalities, the variational principle was used to link the unscaled and scaled systems. If we now use an approximate functional and use its self-consistent densities, the inequalities are automatically satisfied if the previous scaling relationships are true. This makes it more difficult to use these inequalities as exact conditions for functional construction, however work is ongoing to interprete the effect of these inequalities on potential functionals, like those of Ref. [25].

We thank Eberhard Engel for use of the OPMKS code and also thank Cyrus Umrigar for providing exact densities.

3.6 B88 Derivation

As discussed in chapter 2.4.1, the natural successor to LDA is a semi-local (or gradient-corrected) approximation which adds information about the derivative of the density at that point. In fact, in the same paper in which LDA is introduced, so

too is the gradient expansion approximation (GEA) for XC. The coefficients of the GEA are determined by the energy of a slowly-varying gas[13, 14, 57]. However it was found that the GEA often worsened LDA results and two decades passed before substantial improvements were made.

Generalized gradient approximations (GGAs) effectively resum the gradient expansion, but using only $|\nabla n|$. The B88 functional[9] is the most used GGA for exchange overall (as part of B3LYP[10, 58]), but the most popular GGA in solid state applications is PBE[8]. Neither reduces to the GEA in the limit of small gradients. In this paper we explain the reason why this must be the case. Asymptotic expressions for the energy components as functionals of N, the number of electrons, display 'unreasonable accuracy'[59] even for low N. In order to give good energies for finite systems, any approximate XC functional must have accurate coefficients in its large-N expansion. LDA gives the dominant contribution, but the GEA does not yield an accurate leading correction for atoms. Popular GGAs such as B88 and PBE do get this correction right.

In Ref. [29], the underlying ideas behind this work were developed, however the reasoning was based upon scaling the density and not on the potential scaling discussed below. We refine these ideas and explicitly show how they can be used for functional development, and in particular we show how the parameter in B88 may be derived in a non-empirical manner.

Asymptotic expansion in N Begin with any system (atom, molecule, cluster, or solid) containing N electrons. We then imagine changing the number of electrons to N'. Since we usually begin from a neutral system, usually we consider only $N' > N$. Thus we define a scaling parameter $\zeta = N'/N > 1$. As we change the particle number, we simultaneously change the one-body potential $v_{\rm ext}(\mathbf{r})$ as in Eq. (3.1) so as to retain overall charge neutrality. We refer to this as charge-neutral (CN) scaling.

For an isolated atom, $Z \to \zeta Z$ under this scaling, so it remains neutral as the electron number grows. For molecules with nuclear positions $\mathbf{R}_\alpha$ and charges Z_α, $Z_\alpha \to \zeta Z_\alpha$ and $\mathbf{R}_\alpha \to \zeta^{-1/3}\mathbf{R}_\alpha$. In the special case of neutral atoms, the resulting series for the energy is well-known:

$$E = -a_0 N^{7/3} - a_1 N^2 - a_2 N^{5/3} - ... \tag{3.72}$$

where $a_0 = 0.768745$, $a_1 = -1/2$, and $a_2 = 0.269900$ [59, 60]. We say an approximation is large-N *asymptotically exact* to the p-th degree (AEp) if it recovers exactly the first $p+1$ coefficients for a given quantity under the potential scaling of Eq. (3.1). Lieb and Simon[49, 26] showed that Thomas-Fermi (TF) theory becomes *exact* in the limit $\zeta \to \infty$ for *all* systems. TF is exact in a statistical sense, in that TF gives the correct first term of Eq. (3.72), but not the other terms. We say TF is AE0 for the total energy.

A similar expression exists for the exchange component of the energy alone:

$$E_{\rm X} = -c_0 N^{5/3} - c_1 N - ... \tag{3.73}$$

where $c_0 = 0.2208 = 9a_2/11$ and c_1 will be the main topic of this paper. In a similar fashion, Schwinger demonstrated that the local approximation for exchange is AE0, and this coefficient is given exactly by local exchange evaluated on the TF density[59, 60, 50]. However in order to give atomic exchange energies needed for chemical accuracy, any exchange approximation should be at least AE1.

Now suppose we want to make a local approximation for $E_{\rm X}$ but know nothing about the uniform gas. Dimensional analysis (coordinate scaling[27]) tells us that it must

be of the form:

$$E_{\rm X}^{\rm LDA}[n] = A_{\rm X} I, \qquad I = \int d^3r \; n^{4/3}(\mathbf{r}). \tag{3.74}$$

Requiring that this gives the leading contribution to Eq. (3.73) then fixes the value of the constant $A_{\rm X}$. Using any (all-electron) Hartree-Fock atomic code, such as were already available in the 1960's[61], one calculates I for densities running down a particular column of the periodic table and then deduces its dependence on $Z^{5/3}$. A modern alternative is to use the fully numerical OPMKS code[51] using the OEP exact exchange functional to find densities for neutral atoms from $Z = 1$ to $Z = 88$. By fitting, one finds $I = 0.2965 Z^{5/3}$ and hence $A_{\rm X} = -0.7446$. This is remarkably close to the derived result of

$$A_{\rm X} = -\frac{3}{4}\left[\frac{3}{\pi}\right]^{1/3} = -0.7386. \tag{3.75}$$

Thus, without any recourse to the uniform electron gas, we have derived the correct local approximation to $E_{\rm X}[n]$.

This demonstrates that, via asymptotic exactness, the local approximation to exchange is a universal feature of all systems as $N \to \infty$, when scaled appropriately. (In fact, Schwinger only proved this for atoms[59], we know of no proof for arbitrary systems).

Theory

LDA yields the dominant term in *either* the asymptotic charge-neutral expansion ($\zeta \to \infty$) *or* the gradient expansion for the slowly-varying electron gas, $s \to 0$. We next show that, contrary to popular myth, the important expansion is the charge-neutral expansion, *not* the gradient expansion.

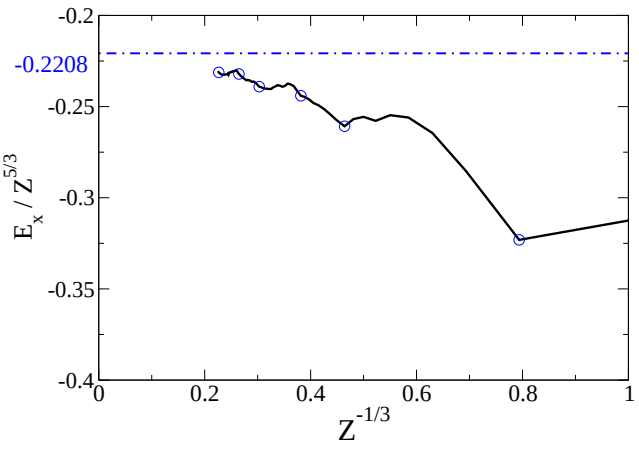

Figure 3.8: The OEP exact exchange energies E_x for neutral atoms from $Z = 1$ to 88, divided by $Z^{5/3}$ in order to pick out the leading term in its asymptotic series. The leading corrections are proportional to powers of $Z^{-1/3}$. The values for the noble gas atoms are given as the circle symbols.

The charge-neutral expansion can be applied to any type of matter, be it molecule or extended solid. For any finite system, the density decays exponentially far from the nuclei. This is a key distinction between finite systems and bulk matter, treated with periodic boundary conditions. Bulk matter has no such regions.

But, for slowly-varying gases, or more generally when there are no classical turning points at the Fermi surface, the charge-neutral scaling and the gradient expansion become identical, i.e., the gradient expansion for the slowly-varying gas is simply a *special case* of charge-neutral scaling. To see that this is so, consider just the kinetic energy as a density-functional. Here the gradient expansion is known out to 6th order[55], and eventually the integrated quantity itself diverges for atomic densities, due to the evanescent tail. But no such divergence occurs for extended systems with finite density everywhere[55, 56].

Thus CN scaling applies to all systems, but only becomes identical to the gradient expansion for slowly-varying bulk systems. For the dominant contribution, effectively the local Fermi wavelength becomes short on the length scale on which the density is

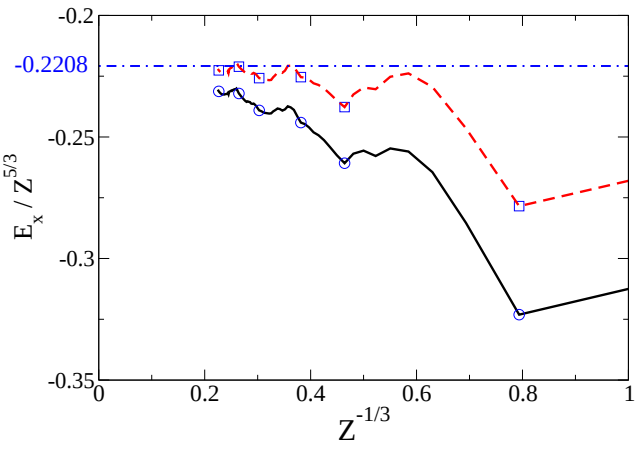

Figure 3.9: We add to Fig. 3.8 the results for the LDA functional evaluated on the OEP densities (dashed-line) keeping the XX values (solid line). As in Fig. 3.8, the Noble gas atom are highlighted with circle and square symbols for XX and LDA respectively.

changing, so that the local approximation applies, and yields the exact answer for this term. Hence LDA reproduces the AE0 terms, but GEA does *not* produce the leading corrections. All this has been amply demonstrated for simple 1d model systems[50], and for the Kohn-Sham kinetic energy for atoms[62].

Here we apply the same reasoning for exchange. The local approximation becomes relatively exact as $\zeta \to \infty$, but the gradient expansion does not reproduce the leading correction in the CN expansion. Below, we use the simple reasoning of Ref. [29] to recover this leading correction. We perform a much more extensive calculation of the asymptotic behavior, using methods developed in Ref. [62]. We find, in agreement with Ref. [29], that the leading correction for atoms is about double that given by the gradient expansion, matching quite closely that of B88 and of PBE. Reversing this logic for B88, we show that B88 may be more or less derived non-empirically via the constraint that the approximation be AE1. If we enforce AE1 exactly, we find a slightly different value for β, and discuss the properties of the resulting functional, excogitated B88.

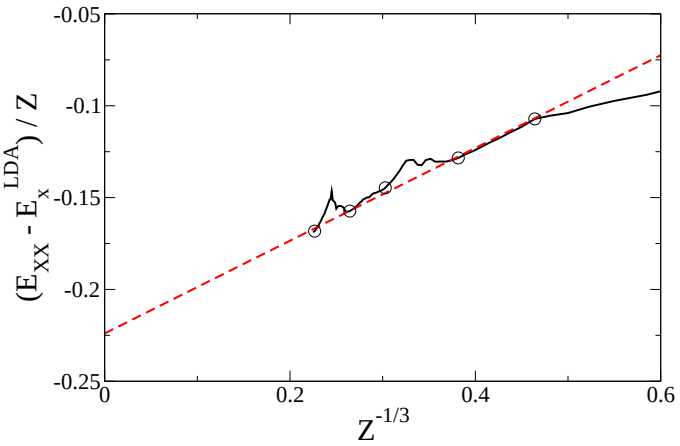

Figure 3.10: We now find the next coefficient in the exchange asymptotic series. To minimize the error due to shell structure oscillations, the LDA exchange energy is subtracted from the exact exchange for each atom. As both give the leading correction, their difference will then have $\Delta c Z$, $\Delta c = c_1 - c_1^{\mathrm{LDA}}$, as the leading term in its asymptotic expansion, . The dashed line is the result of fitting to the noble gas atoms (circle symbols).

Extracting asymptotic coefficients

Under the potential scaling of Eq. (3.1), any approximation for the exchange energy that reduces to LDA in the uniform limit has an expansion in N like Eq. (3.73), with the same value for c_0. However the coefficient c_1 depends on the particular approximation. Below we explain the procedure used to extract these coefficients.

As mentioned in the previous section, the OPMKS[51] electronic structure code is a fully numerical electronic structure code that has the ability to perform optimized effective potential (OEP) calculations. We evaluate the various approximations using atomic densities found with the OEP exact exchange (XX) method. The densities found using this method will be extremely close to the exact densities despite the fact that correlation is missing. Moreover the effect of correlation will contribute at higher orders in the asymptotic expansions of the energy than those we are interested in. Thus EXX calculations are in principle sufficient for extracting the coefficient we

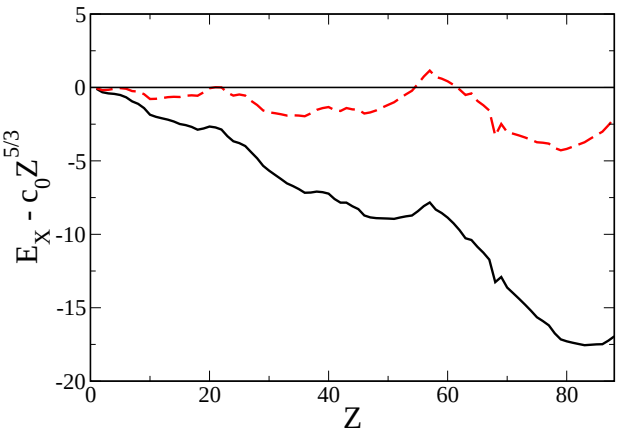

Figure 3.11: In order to see that LDA does not significantly contribute to the higher orders of the exchange asymptotic series, we plot the difference between LDA and the leading term $c_0 Z^{5/3}$ (dashed line), as a function of Z. The exact exchange value is also shown (solid line).

seek.

In Fig. 3.8, we plot $E_{\rm x}/Z^{5/3}$ vs $Z^{-1/3}$ where $E_{\rm x}$ is the exchange energy from the exact exchange calculation. Since the leading term in the asymptotic expansion of Eq. (3.73) is $Z^{5/3}$, this procedure picks out the c_0 coefficient as a constant while all other terms are functions of $Z^{-1/3}$. One can see that the curve in Fig. 3.8 is heading towards the exact value of $c_0 = -0.2208$, but it is difficult to extract higher coefficients due to oscillation of the curve due to the shell structure.

To overcome this difficulty, in Fig.3.9 we add the LDA curve to Fig.3.8. It can be seen that it too recovers the exact c_0 coefficient, but also clearly differs in higher orders in the asymptotic expansion. More usefully, we see that the LDA curve mimics the oscillations shown by exact exchange, so subtracting LDA from EXX will minimize this effect and make the extraction of asymptotic coefficients more accurate.

In Fig. 3.10, we plot $(E_{\rm x} - E_{\rm x}^{\rm LDA})/Z$ vs $Z^{-1/3}$ and find that it behaves close to linearly. There appears to be no $Z^{4/3}$ term in $E_{\rm x}$. Such a contribution was argued

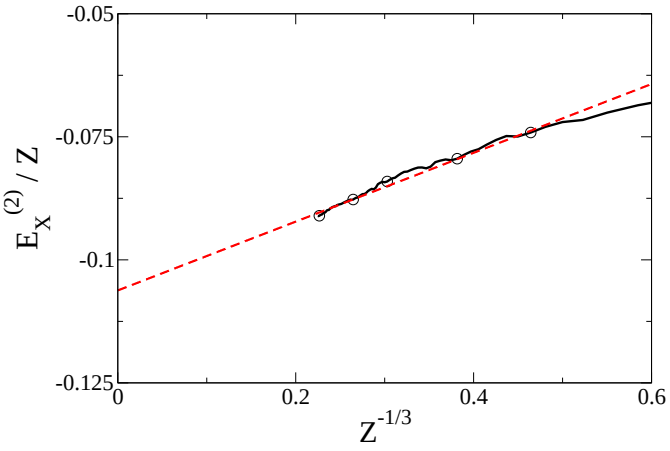

Figure 3.12: We use the same procedure as in Fig. 3.10 to find the Δc coefficient for the gradient correction to LDA, $E_{\rm X}^{(2)}[n]$, as defined in Eq. (2.49). The dashed line was fitted to the noble gas atoms (circle symbols).

not to exist in Ref. [29], but this was based on CN scaling of the density and studying the behavior of the terms in the gradient expansion. That reasoning is insufficient, as the expansion should be performed in terms of the potential, as described in Sec. 3.6. But since the Scott correction (the Z^2 contribution to the total energy) comes from the core region, there is no reason to expect an analogous contribution for exchange. In order to show this and also to precisely determine the c_1 coefficient, one should use the techniques developed by Schwinger for deriving the Scott correction to the total energy[59], but apply them to exchange.

To further reduce the remaining uncertainty due to shell structure oscillations, we choose simply to use the noble gas atoms (excluding helium) for our fit. The strongest deviations from linearity come from the transition metals and lanthanides and actinides. We fit the difference $(E_{\rm X} - E_{\rm X}^{\rm LDA})/Z$ with a straight line in $Z^{-1/3}$, and extrapolate to $Z \to \infty$, finding $\Delta c = -0.2240$, where $\Delta c = c_1 - c_1^{\rm LDA}$, and

$$E_{\rm X} \approx E_{\rm X}^{\rm LDA} - 0.2240\, Z + 0.2467\, Z^{2/3}. \tag{3.76}$$

The coefficient of the last term is given by the slope of the dashed line in Fig. 3.10, although the meaning of this term is unclear in the presence of such strong oscillating

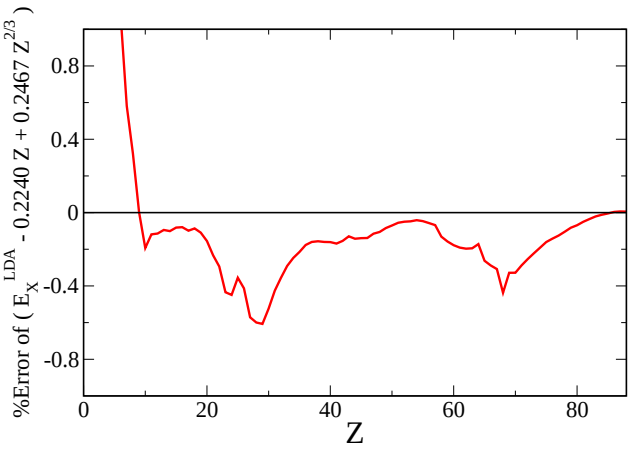

Figure 3.13: The percentage error of the approximate asymptotic series given in Eq. (3.76) is plotted as a function of Z. The error is remarkably low and demonstrates the power of these asymptotic series.

If instead we used the alkaline earth atoms (excluding beryllium), we find an almost identical value, $\Delta c = -0.2236$. If we use all elements with $Z > 10$, we find a similar value, $\Delta c = -0.2164$. If all elements from $Z = 1$ to 88 are used, we find $\Delta c = -0.1982$. In Ref. [29], Δc was found using noble gas atoms, except with the helium value included, and that method gave a value of $\Delta c = -0.1978$. In our analysis, atoms with $Z < 10$ are not used as they are not necessarily dominated by the asymptotic series.

Since LDA displays the shell oscillations that prevented us from fitting EXX directly, the value of the LDA c_1 coefficient cannot be found exactly. But we estimate $0 \geq c_1^{\mathrm{LDA}} \geq -0.04$, i.e., at least five times smaller in magnitude than Δc. In Fig 3.11, we show $E_{\mathrm{x}} - c_0\, Z^{5/3}$ as a function of Z for both the exact values and within LDA, demonstrating that the linear contribution comes almost entirely from the beyond-LDA terms.

Finally we determine Δc for GEA. In Fig. 3.12, we plot $(\mathrm{E_X^{GEA}} - E_\mathrm{X}^\mathrm{LDA})/Z$ vs $\mathrm{Z}^{-1/3}$ in order to find $\Delta c = c_1^\mathrm{GEA} - c_1^\mathrm{LDA}$, finding $\Delta c = -0.1062$. This plot is much closer to linear than the previous one. The leading corrections to LDA in the asymptotic expansion produce corrections to the shell structure *beyond* those captured by LDA evaluated on the exact density [50, 62]. Although the smooth contribution can be partially captured by GEA, there is almost no correction to the shell structure. Just as for the kinetic energy[62], GEA yields a correction to the smooth part that is about

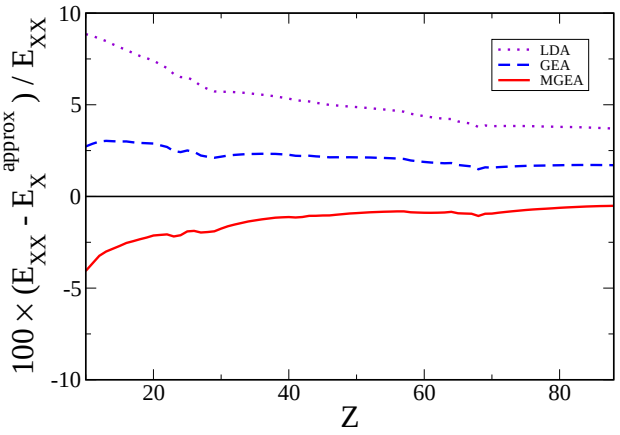

Figure 3.14: The percentage error for LDA, GEA and the modified GEA (MGEA) exchange functionals for $Z > 10$. The coefficient of $E_\mathrm{X}^{(2)}$ is multiplied by 2.109 in order to make the MGEA AE1 asymptotically exact.

To understand the power of these asymptotic expansions, we add the corrections of Eq. (3.76) to the LDA energies, and in Fig. 3.13 plot the percentage error relative to exact exchange, as a function of Z. For all but the second row of the periodic table, the resulting error is below 0.5% in magnitude, and typically of order 0.2%.

Generalized gradient approximations

Generalized gradient expansions were designed to improve energetics over LDA for electron systems of interest and relevance. Early versions, such as PW91[63, 64], were

Table 3.3: $\Delta c = c_1 - c_1^{\mathrm{LDA}}$ values for several different functionals.

	E_X	LDA	GEA	B88	PBE
Δc	-0.2240	-	-0.1062	-0.2216	-0.1946

tortured into reducing to the gradient expansion when the density is slowly varying. But this was later given up, in both B88 and PBE exchange, which both reduce to the gradient expansion form for slow variations, but with coefficients much larger than that of the gradient expansion.

Our analysis explains why this must be so. Regardless of its derivation, any modern GGA for exchange is tested against the neutral atoms. Any approximation that cannot recover the right c_1 will be generally inaccurate for these energies, and so discarded. Thus any that become popular have already passed this test.

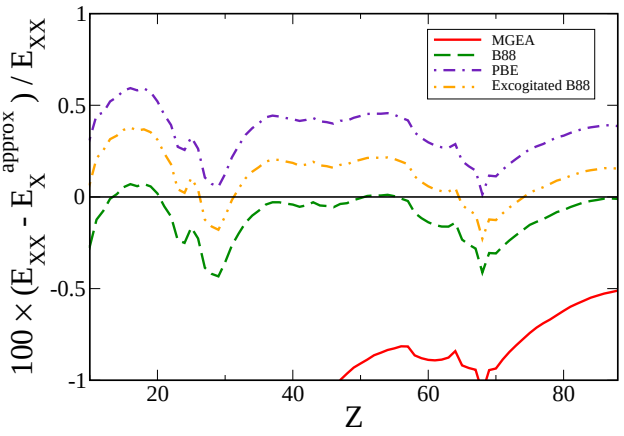

Figure 3.15: We add to Fig. 3.14 the results for B88, PBE, and the excogitated B88 functional, all evaluated on the OEP exact exchange densities.

In Table 3.3, we give the results for Δc for several different functionals. The same methodology was used in all extractions. Both popular GGA's recover (at least approximately) the accurate value. B88, designed specifically for molecular systems, is very close to the accurate value. PBE exchange is less so, but is also designed to bridge molecular and solid-state systems. The PBE value is between that of GEA and B88,

but much closer to the latter than the former. Taking advantage of this insight, a new variation on PBE, called PBEsol[45], restores the original gradient expansion, thereby worsening atomization energies (total energy differences), but improving many lattice constants of solids over PBE and LDA.

Deriving the β in B88

The exchange energies found using GGAs such as B88 or PBE are generally dominated by their gradient expansion components for most chemically relevant densities. Thus, to make B88 AE1, it is sufficient to impose this exact condition on just the $E_{\rm X}^{(2)}[n]$ functional form. Since both B88 and the GEA are built on top of LDA, we can simple look at the Δc values calculated above. If we set $\mu = 2.109\mu_{\rm AK}$ in Eq. (2.49), we multiply the c_1 coefficient of GEA by a factor of 2.109, making it AE1. In Fig. 3.14, we name this functional MGEA for modified GEA and plot its percentage errors. The values for LDA and GEA are also shown. It can be seen that modifying GEA to be AE1 has greatly reduced the error.

We now require that the B88 functional form, Eq. (2.52), reduce to this MGEA for small values of x. Using Eq. (2.51), this corresponds to using a value of $\beta = 0.0050$. Thus we have derived an excogitated B88 that is free of any empirical parameters. The actual value used in B88 is $\beta^{\rm B88} = 0.0053$ (for spin-polarized systems this becomes 0.0042, which is the value given in Ref. ([9])), so the values are very close. This is not surprising as fitting to Hartree-Fock exchange energies is an approximate way of demanding asymptotic exactness. Interestingly, the value quoted as the high-Z asymptote in Ref. [9] and found using Ref. [15] is essentially the same as our value, but was evidently rejected in favor of a better fit. In Fig. 3.15, we plot the percentage errors for B88, PBE, and the excogitated B88. As is typical for empirically-fitted functionals, B88 performs very well for systems close to the data set used in the fitted procedure. Although the error for PBE is higher than both B88 and the excogitated

B88, it is systematic in its overestimation. As noted, PBE was designed to perform reasonably well for a wide range of systems, so again its behavior is not surprising. On this data set, the excogitated B88 was never going to do better than B88, although it remains to be seen how it performs for more complicated systems.

conclusion

We have carefully and systematically extracted the leading large-Z correction to the exchange energy of atoms. Our results differ slightly from those of Ref. [29] but yield the same qualitative conclusion, i.e., that the gradient expansion yields an error of a factor of 2 or more for this coefficient. We have clarified some of the reasoning, and applied it more generally to any atom, molecule, or cluster. By looking in detail at the exchange energy asymptotic series for neutral atoms, we have demonstrated the power of using such series for functional development. Requiring that the small gradient expansion of B88 capture the two leading coefficients of the asymptotic expansion is a method by which the unknown coefficient β can be found. This gives a coefficient very close to the one actually used in B88 and thus is an *ex post facto* 'derivation' of B88. Inserting our most accurate estimate for β into the B88 form yields an excogitated B88.

We thank Eberhard Engel for the use of his atomic OPMKS code, and NSF CHE-0809859 .

3.7 Implications for DFT

So what does this mean for modern electronic structure theory? Most importantly, this work unites rigorous proofs about TF theory[26], Schwinger's semiclassical results for neutral atoms[22], and modern functional development for KS calculations.

Exchange: We have shown that the local approximation to exchange becomes exact as $\zeta \to \infty$ for all systems, consistent with the fact that all popular functionals recover this limit. Furthermore, to be AE1 for $E_{\rm x}$ of atoms, their small gradient limit must be about double that of the gradient expansion[29], and this is also true for both empirical[9] and non-empirical functionals[8]. These functionals agree for moderate gradients, and differ for large gradients. For periodic systems without turning points, the gradient expansion is AE to the order of the gradients. Restoring the original gradient expansion greatly improves lattice parameters[24]. Finally, recent beyond-GGA functionals that recover the 4th-order gradient expansion yield good approximations for the enhanced gradient coefficient in atoms[29].

To apply the methods developed here directly to atoms, we need to generalize them to include turning points, evanescent regions, and Coulomb cores. Such a scheme might produce a derivation of an GGA beyond the small gradient limit.

Correlation: As the behavior of $E_{\rm c}$ is not governed by a simple asymptotic expansion[29], we have not found a universal limit in which local correlation becomes exact. Consistent with this, most non-empirical $E_{\rm c}$ functionals are designed to be exact when the density is uniform[8], but this condition is violated by empirical functionals[10].

Now $E_{\rm xc}$ for a large jellium cluster is dominated by a bulk contribution (exact in LDA), and a surface contribution, which can be accurately approximated by a GGA. Restoring the density-gradient expansion for $E_{\rm x}$ in PBE yields a highly accurate surface exchange energy, so the analog is to recover the surface correlation energy[24].

KS kinetic energy: A holy grail for many years[65] has been to find an accurate kinetic energy functional, $T_{\rm s}[n]$, bypassing the construction of KS orbitals. Almost all approaches begin from a semilocal expression, sometimes enhanced by non-locality based on linear response. This study shows that, if one is interested in total energies,

a vital feature is to be asymptotically correct for neutral atoms. Thus, as $\zeta \to \infty$ in either potential- or density-scaling, the functional *must* reduce to TF. For atoms, the gradient expansion of $T_{\rm S}[n]$ works rather well. The coefficient of Z^2 is -0.65 in TF theory, -0.53 if $T^{(2)}$ is included, and -0.52 if $T^{(4)}$ is added [53]. Thus each succesive term in the gradient expansion brings it closer to being AE1, since the exact value is -1/2. Generalizing the gradient expansion to make it AE2 produces a more accurate functional for total energies of both atoms and molecules[53]. Lastly, our example here shows how much simpler the kinetic energy is as a functional of the potential than of the density.

Chapter 4

Partition Density Functional Theory

In the world of electronic structure, molecules and solids are typically considered in one of two distinct ways. In the first, the system is treated as a whole and molecular orbitals (or bloch wavefunctions for bulk solids) are calculated. These are solutions of some effective potential theory, such as Kohn-Sham[1, 2] density functional theory or Hartree-Fock[66, 67], and often describe well the system near equilibrium geometries. The major difficulty is then finding usefully accurate approximations to the total energy. In the second view, one considers isolated atoms as the starting point, and then weak interactions between such units. This view appears necessary for strongly-correlated solids such as NiO, strongly-correlated molecules such as Cr_2, or any molecule as its bonds are stretched. In such cases, standard approximations for the single-reference approach usually fail, often quite completely. Thus the worlds of weak- and strong-correlation have practically divided[68].

In this work, we show that the partition theory of Ref. [69] plays a role analogous to

that of the Kohn-Sham formalism in density functional theory (DFT). In Kohn-Sham theory[2], a reference system is created which is much easier to solve and in which the interactions between electrons have been turned off. In partition theory[69, 70], the reference system has been constructed from effective isolated fragments (e.g., atoms) between which there are no interactions. In both theories, the total electronic density of the system is used as the connection between reference and reality: it remains unchanged from one to the other, and so uniquely defines the reference. Many other analogies are made within the paper. Suffice to say that, just as KS DFT is particularly well-suited to weakly-correlated systems, partition theory works best for weakly interacting fragments.

I start with the relevant background information on partition theory. Following this, density functional partition theory (PDFT) is formally introduced, before being analyzed in detail. Next I illustration PDFT on three different systems, each highlighting a feature of PDFT. The point of these illustrations is to show that PDFT is an exact theory and will provide the exact molecular energy and molecular density at self-consistency.The first system studied is a homonuclear diatomic molecule. This system is also used to demonstrate partition theory, so we can see the PDFT converge to the PT results. Next we move to the more complecated case of a heteronuclear diatomic molecule, which creates non-symmetric charges on the two atoms. In both of these examples, neutral diatomic molecules are used as the kinetic energy density functional is known analytically for two or less fermions, in the final example I study a 12 atom, 12 fermion chain. This example is much more complicated, but is still solved exactly.

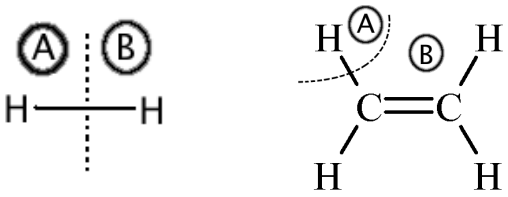

Figure 4.1: Two examples of binary fragmentation into fragments A and B. The figure on the left shows a hydrogen molecule at equilibrium bond length, while on the right, an ethene molecule is shown with one substituent cornered off as a fragment.

4.1 Partition Theory

Partition theory[69] provides a method for breaking a system into a sum of fragments. Begin from the one-body potential, $v(\mathbf{r})$, which is typically a sum of contributions, most from individual nuclei; e.g.

$$v(\mathbf{r}) = -\sum_{\beta} \frac{Z_\beta}{|\mathbf{r} - \mathbf{R}_\beta|} \quad , \tag{4.1}$$

where Z_β is the atomic charge of a nucleus at point $\mathbf{R}_\beta$. In partition theory, we group these contributions into N_f fragments of our choosing:

$$v(\mathbf{r}) = \sum_{\alpha=1}^{N_f} v_\alpha(\mathbf{r}) \quad , \tag{4.2}$$

and each $v_\alpha(\mathbf{r})$ is the sum over one or more nuclei. The simplest possible choice is to divide the system into two parts (N_f=2), which we call binary fragmentation. These parts would obviously be the two nuclei in a diatomic molecule, but could also be the nuclei of a chemical group extracted from a large molecule, or those of a molecule interacting with a surface. One can imagine many examples that could prove useful, examples of which can be seen in Fig. 4.1. An alternative choice is atomization, in which every term in Eq. (4.1) above is separated, and the number of fragments matches the number of nuclei.

Once the fragments have been picked, the partition problem is to find fragment densities $n_\alpha(\mathbf{r})$ such that they add to the total molecular density:

$$\sum_{\alpha=1}^{N_f} n_\alpha(\mathbf{r}) = n(\mathbf{r}) \quad . \tag{4.3}$$

Within partition theory, this is done by minimizing the total energy of the fragments, E_f, with the constraint that the sum of the fragment densities must match the molecular density, i.e. Eq. (4.3). The total energy of the fragments is

$$E_f = \sum_{\alpha=1}^{N_f} \epsilon_\alpha \quad , \tag{4.4}$$

where ϵ_α is the energy of each fragment. Since there is no constraint that a fragment's particle number, N_α, be an integer, the PPLB formulation[71, 72] is used. Thus

$$\epsilon_\alpha = (1-\nu_\alpha)E_\alpha[n_{p_\alpha}] + \nu_\alpha E_\alpha[n_{p_\alpha+1}] \tag{4.5}$$

and

$$n_\alpha(\mathbf{r}) = (1-\nu_\alpha)n_{p_\alpha} + \nu_\alpha n_{p_\alpha+1} \tag{4.6}$$

where

$$E_\alpha[n] = F[n] + V_\alpha[n] = F[n] + \int d^3r\, n(\mathbf{r})\, v_\alpha(\mathbf{r}) \tag{4.7}$$

is the energy density functional for each fragment α. The fragment particle number is $N_\alpha = p_\alpha + \nu_\alpha$, p_α and $p_\alpha + 1$ are the lower and upper bordering integers of N_α and $0 \leq \nu_\alpha < 1$. The PPLB scheme is simply that of the fragment in contact with an infinite but distant reservoir.

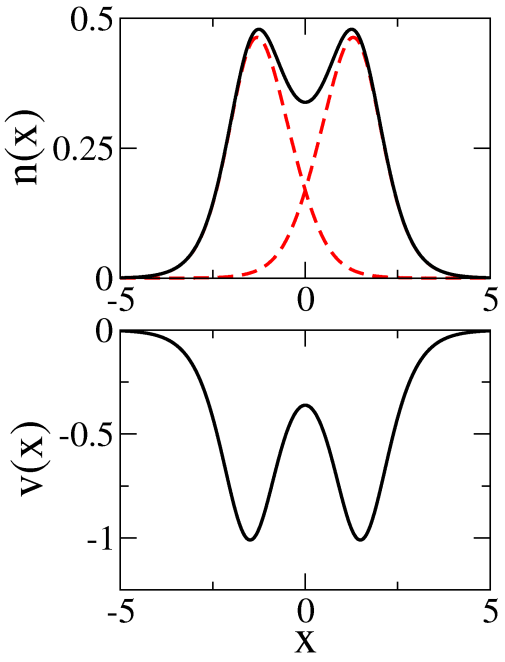

Figure 4.2: Top panel: The exact density (solid line) for two non-interacting fermions in the potential defined in Eq. (4.19) with $R = 3$ and shown below. The two exact partition densities (dotted lines) for this system. Bottom panel: The corresponding molecular potential (solid line) as defined in Eq. (4.19).

We note the following:

- if all fragments are separated from each other, these fragment densities become exactly those of the isolated fragments, $n_\alpha^{(0)}(\mathbf{r})$.
- One solves the Hamiltonian for each isolated fragment independently of the other fragments. It is the sum of these fragment energies that is minimized.
- In principle finding the minimum requires first solving for the molecular density, and so is even more work than solving the initial problem. But an exactly analogous statement can be made about KS DFT.

The process of finding the minimum produces an extremely useful conceptual tool.

Minimizing the Lagrangian:

$$\mathcal{G} = E_f - \mu \left(\sum_{\alpha=1}^{N_f} \int d^3r \; n_\alpha(\mathbf{r}) - N \right) + \int d^3r \; v_p(\mathbf{r}) \left(\sum_{\alpha=1}^{N_f} n_\alpha(\mathbf{r}) - n(\mathbf{r}) \right) \quad (4.8)$$

yields the solution to the partition problem[69]. The Lagrange multiplier μ is identified as the chemical potential, while the Lagrange multiplier that constrains the sum of the fragment densities to be the molecular density is a potential, dubbed the partition potential, $v_p(\mathbf{r})$. This is a global property of the molecule, uniquely defined once we have chosen a particular fragmentation. It has the interesting aspect that, when added to any fragment potential, the sum is exactly that potential for which the fragment density is a ground state density. In the upper panel of Fig. 4.2, the exact total density for a model system is shown. It is the solution for two non-interacting fermions in the potential shown in the lower panel of Fig. 4.2 and is discussed in detail in Sec. 4.3. Solving the partition problem yields the two fragment densities, which are also shown in the upper panel of Fig. 4.2. It can be seen that adding these two fragments densities will give the total density. In the lower panel of Fig. 4.3, we show the exact partition potential for this problem. When added to a fragment potential, it gives an effective potential for each fragment, this is shown as the dotted line in the lower panel of Fig. 4.3. The ground-state density of this effective potential can be seen in the upper panel of Fig. 4.3, it is exactly the same as the fragment density shown in the upper panel of Fig. 4.2.

We emphasize here that once a choice of fragmentation has been made, the entire procedure is then unambiguously defined, and leads to unique fragments. The user chooses fragments depending on which aspects they wish to study, usually guided by chemical intuition.

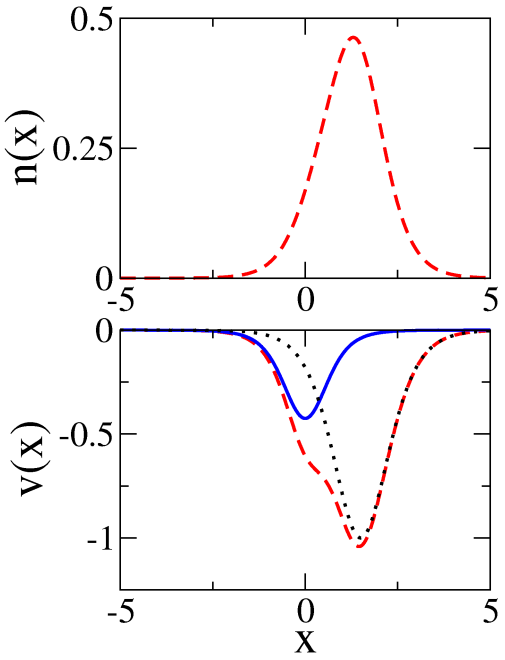

Figure 4.3: Top panel: The fragment density (dotted line) for the B atom of Fig. 4.1. Bottom panel: The exact partition potential $v_p(x)$ (solid line) for this system, the nuclear potential $v_B(x)$ (dotted line), and the fragment potential $v_B(x) + v_p(x)$ (dashed line). This potential has the fragment density shown in the upper panel as its ground state density.

4.2 Partition density functional theory

In this section, we develop a methodology which allows one to *calculate a molecular density and energy from individual calculations on fragments*, via a self-consistent loop. In this sense, it is the analog of the KS method, in which the energy is found from self-consistent calculations on non-interacting electrons. Clearly such a capability in general could have tremendous significance for many areas of current research, from $O(N)$ scaling to QM/MM methods.

To do so, think of the total fragment energy, Eq. (4.4), as analogous to the KS energy of Eq. (2.39). Then define the partition energy as

$$E_p = E - E_f, \tag{4.9}$$

analogous to Eq. (2.40), the Hartree-XC energy in KS theory. If $E_f^0 = \sum_\alpha \epsilon_\alpha^0$ is the total energy of the isolated fragments, then we can write

$$E_p = E_{dis} + E_{rel}, \tag{4.10}$$

where E_{rel} is the fragment relaxation energy:

$$E_{rel} = E_f^0 - E_f \tag{4.11}$$

and $E_{dis} = E - E_f^0$, is the dissociation energy. For any bound molecule, $E_{dis} < 0$. Furthermore, since E_f^0 is the ground state energy for the isolated fragments system, $E_f > E_f^0$. Thus $E_p < 0$ and is expected to be much smaller than the total energy (on the scale of chemical bonding), and vanishes as the fragments are pulled apart.

We can consider the partition energy as a functional, $E_p[\{n_\alpha\}]$, of the fragment densities alone, for the given external potential and choice of fragmentation. Now, we examine the effect of making small variations in one fragment density, $\delta n_\alpha(\mathbf{r})$, to the partition energy. The first term of Eq. (4.9) is the ground-state energy of the system, so variations in the density are zero, because we are at its minimum. For E_f, the second term, only the α-th fragment energy changes. Since the fragment density minimizes the α-th fragment in the presence of $v_p(\mathbf{r})$, then $v_p(\mathbf{r}) = \delta\epsilon_\alpha/\delta n_\alpha(\mathbf{r})$, so that

$$v_p(\mathbf{r}) = \frac{\delta E_p[\{n_\alpha\}]}{\delta n_\alpha(\mathbf{r})}, \tag{4.12}$$

i.e., given any expression for $E_p[\{n_\alpha\}]$, we can extract the corresponding partition potential, $v_p(\mathbf{r})$, and then calculate new fragment densities, which are then used to generate a new partition potential, and so on. Thus approximating $E_p[\{n_\alpha\}]$ produces a closed loop, and a direct scheme for doing a PDFT calculation. The steps of a PDFT

calculation are:

1. Guess the fragment densities $\{n_\alpha\}$. A reasonable guess would be $\{n_\alpha^0(\mathbf{r})\}$, the densities of the isolated fragments.

2. The fragment charges, $\{N_\alpha\}$, are determined by the fragment chemical potentials.

3. Construct the partition potential, $v_p(\mathbf{r})$, using Eq. (4.12).

4. Solve for each $n_\alpha(\mathbf{r})$ in its respective fragment potential $v_\alpha(\mathbf{r}) + v_p(\mathbf{r})$.

5. Cycle steps 2, 3 and 4 until self-consistency.

6. Along with the fragment densities, this yields the total molecular density and the molecular energy (via $E = E_f + E_p$).

In principle, any electronic structure method can be used to calculate the fragments. However, in practice, most of such methods will not provide a way to functionally differentiate the corresponding E_p. Even within KS DFT, one does not usually know the non-interacting kinetic energy, T_s, as a functional of the density. Only with an explicit density functional can the corresponding derivative needed for the partition potential be taken.

To derive an expression for $v_p(\mathbf{r})$, we write $E_p[n]$ in terms of DFT quantities:

$$E_p[n] = F[n] - \sum_{\alpha=1}^{N_f} F[n_\alpha] + \sum_{\alpha=1}^{N_f} \sum_{\beta\neq\alpha}^{N_f} \int n_\alpha(\mathbf{r}) v_\beta(\mathbf{r}). \tag{4.13}$$

For simplicity, we assume N_α is an integer, otherwise Eq. (4.5) must be used. so we can write the partition potential in terms of functional derivatives of the universal

functional:

$$v_p(\mathbf{r}) = \frac{\delta F[n]}{\delta n(\mathbf{r})} - \frac{\delta F[n_\alpha]}{\delta n_\alpha(\mathbf{r})} + \sum_{\beta\neq\alpha}^{N_f} v_\beta(\mathbf{r}) \quad . \tag{4.14}$$

This gives an expression for $v_p(\mathbf{r})$ for each of the N_f fragments. Using the fact that the universal function can be decomposed into $F[n] = T_{\rm S}[n] + U[n] + E_{\rm XC}[n]$, this leads to

$$v_p[\{n_\alpha\}](\mathbf{r}) = \frac{\delta T_{\rm S}[n]}{\delta n(\mathbf{r})} - \frac{\delta T_{\rm S}[n_\alpha]}{\delta n_\alpha(\mathbf{r})} + v_{\rm XC}[n](\mathbf{r}) - v_{\rm XC}[n_\alpha](\mathbf{r}) + \sum_{\beta\neq\alpha}^{N_f} \left(v_\beta(\mathbf{r}) + v_{\rm H}[n_\beta](\mathbf{r})\right) \tag{4.15}$$

for any α, and using the fact that the Hartree potential is linear in $n(\mathbf{r})$. Explicit density functional expressions are needed for both $T_{\rm S}[n]$ and $E_{\rm XC}[n]$. However since the expression only depends on differences between the functional derivatives of these, some of the error due to approximating these may cancel.

To find the fragment occupations, note that at self-consistency, the chemical potentials of all the fragments will be equal. We choose $N_\alpha^{(k+1)} = N_\alpha^{(k)} - \Gamma\left(\mu_\alpha^{(k)} - \bar{\mu}^{(k)}\right)$, where Γ is another positive constant and $\bar{\mu}$ is the average of the fragment chemical potentials, used in conjunction with Eq. (4.5) for the functionals.

If we use DFT to perform the fragment calculation, the KS potential for the α-th fragment is found from Eq. (4.12) in KS quantities:

$$v_{{\rm S},f,\alpha}[n_\alpha, \bar{n}_\alpha](\mathbf{r}) = v_{\rm S}[n_\alpha](\mathbf{r}) + \left(v(\mathbf{r}) + v_{\rm HXC}[n](\mathbf{r}) - v_{\rm S}[n](\mathbf{r})\right), \tag{4.16}$$

where $v_{\rm S}[n](\mathbf{r}) = -\delta T_{\rm S}[n]/\delta n(\mathbf{r})$, and $n(\mathbf{r}) = n_\alpha(\mathbf{r}) + \bar{n}_\alpha(\mathbf{r})$. This is the central result of this paper, as it gives the fragment KS potential for a pair of trial densities, $n_\alpha(\mathbf{r})$ and $\bar{n}_\alpha(\mathbf{r})$, in terms of quantities from KS-DFT.

4.3 Homonuclear Diatomic Molecule

For one or two electron systems, the kinetic energy density functional is given exactly by the von Weizsäcker functional:

$$T_{\rm W}[n] = \frac{1}{8}\int d^3r\ \frac{|\nabla n(\mathbf{r})|^2}{n(\mathbf{r})}\quad , \tag{4.17}$$

and if we study non-interacting fermions, then $E_p[n]$ as a density functional is known exactly. Taking the functional derivative with respect to a fragment density yields the partition potential, which for a binary fragmentation of a symmetric system is:

$$v_p(\mathbf{r}) = v_B(\mathbf{r}) + \left(\frac{n'^2(\mathbf{r})}{8n^2(\mathbf{r})} - \frac{n''(\mathbf{r})}{4n(\mathbf{r})}\right) - \left(\frac{n_A'^2(\mathbf{r})}{8n_A^2(\mathbf{r})} - \frac{n_A''(\mathbf{r})}{4n_A(\mathbf{r})}\right) \tag{4.18}$$

in the absence of electron interaction. For a non-symmetric system, the general formalism[71] for non-integer particle number must be used. If we work in one dimension, then the 1-fermion fragments can be solved easily.

For this example, we use a $1/\cosh^2(x)$ potential for the each 'nucleus', giving the total potential for a diatomic system with separation R as:

$$\begin{aligned} v(x) &= v_A(x) + v_B(x) \\ &= -\frac{1}{\cosh^2(x-R/2)} - \frac{1}{\cosh^2(x+R/2)}. \end{aligned} \tag{4.19}$$

In Fig. 4.4, we show the convergence for one of the two fragment densities for this

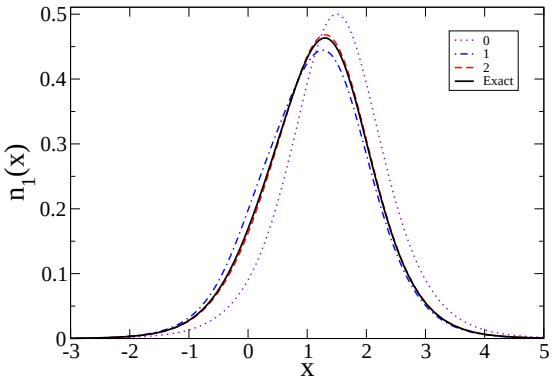

Figure 4.4: The density for the left (A) fragment as defined by Eq. (4.19) with $R = 3$ for the first 3 self-consistency cycles, labelled $0, 1, 2$ respectively. Also shown is the exact fragment density from a partition theory calculation. Even after just 2 cycles, the fragment density is almost on top of the exact density, on this scale. For more self-consistency steps, it continues converging towards the exact answer. Calculations were performed using 3-site finite difference formulas for derivatives and 2001 grid points with a grid spacing of 0.013a.u.

problem, thought several self-consistency cycles. The total potential is the same as that shown in the lower panel of Fig. 4.7, while the two fragment potentials, $v_A(x)$ and $v_B(x)$, are given in Eq. (4.19) with $R = 3$. For the initial fragment densities(cycle 0), we use the densities for the two isolated fragments. We then use these to construct a partition potential from Eq. (4.18), which is then used to construct effective fragment potentials, $v_\alpha(x) + v_p(x)$. If we then solve for each fragment density in this new potential, we find the cycle 1 density, shown as the dot-dashed line in Fig. 4.4. It can be seen that some of the density for this fragment has been shifted towards the other 'nuclei', as compared the isolated case. This is due to the partition potential lowering the fragment potential, v_A, so as to move density into the bonding region, as would be expected.

In Fig. 4.5, the total density, i.e., the sum of the two fragment densities, is shown. The exact molecular density for this problem is also given, it is found by directly solving for two non-interacting fermions in total potential $v(x)$. In both this case and for the fragments, the density is found by solving the Schrödinger equation numerically on a

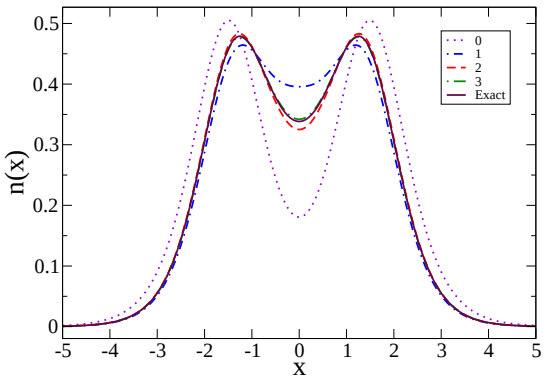

Figure 4.5: Total densities for various cycles $0, 1, 2, 3$ of the self-consistency calculation for this system. Also shown is the exact density for the full system. The density after just 2 cycles is very close to the exact density and after 3 cycles it cannot be distinguished from the exact density on this scale. Convergence continues at more cycles are added. Since the two fragment densities are added together, deviations from the exact result can be seen more clearly for the total density.

real space grid. Derivatives of the density are found using a finite-difference scheme. Similar to the fragment density, we see convergence towards the exact result, however we also include the result after the 3^{rd} cycle as summing the fragment densities amplifies their individual errors. In Fig. 4.6, we show the density differences from the overlapped 'atomic' densities. Clearly the calculation converges to the exact molecular density.

The energy of the molecule may also be calculated using Eq. (4.9) for each set of fragment densities. Again we see the calculation converge to the exact energy of -1.22008. The energy of the initial guess was -1.17854, while after 3 cycles, it was -1.22006, essentially converged for this level of calculation .

4.4 Heteronuclear Diatomic Molecule

In the previous section, we illustrated PDFT on a model system of a homonuclear diatomic molecule. We found, as expected, that PDFT gave exactly the right en-

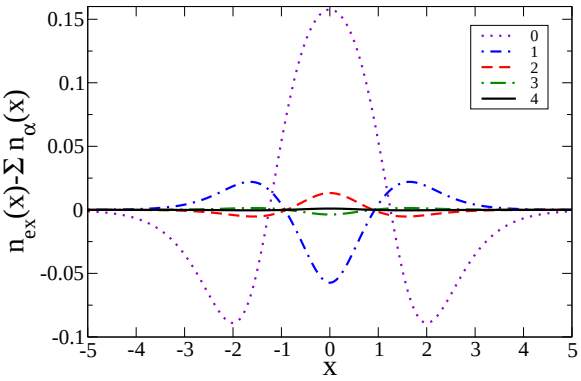

Figure 4.6: Difference between the exact molecular density, $n_{\rm ex}(x)$, and the sum of the fragment densities for each self-consistency cycle of the PDFT calculation. It is the difference between each of the PDFT densities in Fig. 4.5 and the exact density. After each cycle this difference decreases and the convergence to the exact answer is clear.

ergy and density. While this demonstrated the principle of PDFT, a more powerful example of its usefulness and relevance to real systems is a heteronuclear diatomic molecule. Unlike the symmetric case, the covalently-bonded fragments will contain fractional numbers of electrons, necessitating the use of PPLB formalism[71]. In partition theory, the AB heteronuclear system has been studied[73] for insight into molecular dissociation.

For this example, we use a $1/\cosh^2(x)$ potential for each 'nucleus', giving the total potential for a diatomic system with separation R as:

$$v(x) = v_A(x) + v_B(x) = -\frac{1}{\cosh^2(x+R/2)} - \frac{1.1}{\cosh^2(x-R/2)}. \tag{4.20}$$

Here, the A fragment plays the role of a Lewis base while B is a Lewis acid. The small difference in nuclear charges is choosen so as to mimic the effect of screening in an interacting system. The total particle number is two, allowing us to use the von Weizsäcker functional even when fractional charges are present.

The minimization of the Lagrangian, Eq. (4.8), in the partition problem is over both

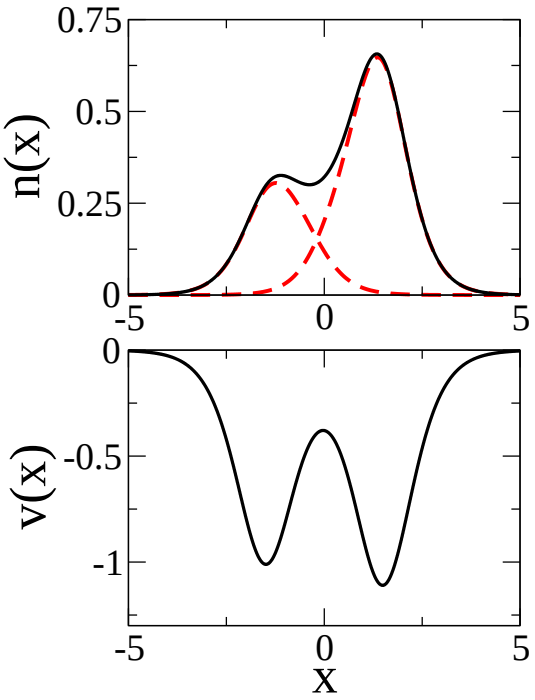

Figure 4.7: Top panel: The exact density (solid line) for two non-interacting fermions in the potential defined in Eq. (4.20) with $R = 3$ and shown below. The two exact partition densities (dashed lines) for this system. Bottom panel: The corresponding molecular potential (solid line) as defined in Eq. (4.20).

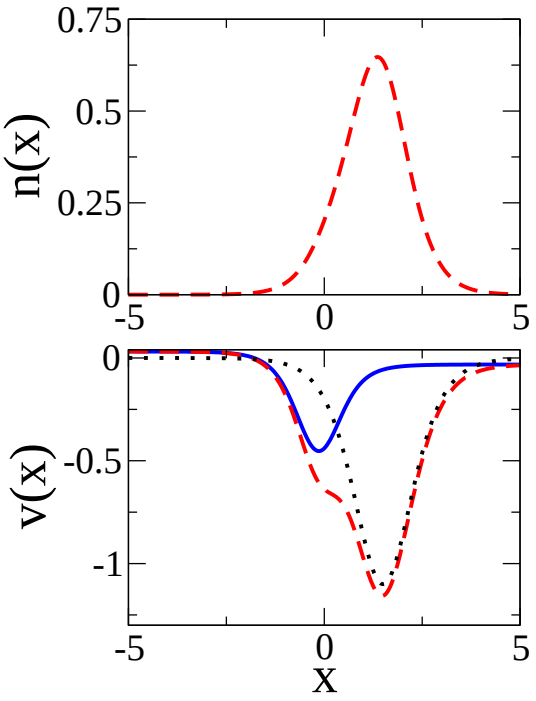

Figure 4.8: Top panel: The fragment density (dashed line) for the B atom of 4.1. Bottom panel: The exact partition potential $v_p(x)$ (solid line) for this system, the nuclear potential $v_B(x)$ (dotted line), and the fragment potential $v_B(x)+v_p(x)$ (dashed line). This potential has the fragment density shown in the upper panel as its ground state density and the same is true for the A atom.

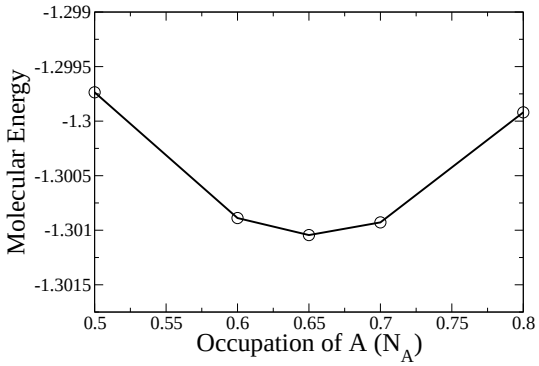

Figure 4.9: The molecular energy after 3 iteration cycles as a function of the fractional occupation of the A fragment (N_A) used in each PDFT calculation. The occupation on B is thus $2-N_A$. The initial fragment densities are the same for each calculation and are simply those of the respective free fragments. The minimum occurs at $N_A = 0.655$, which is then the occupation used in all subsequent calculations.

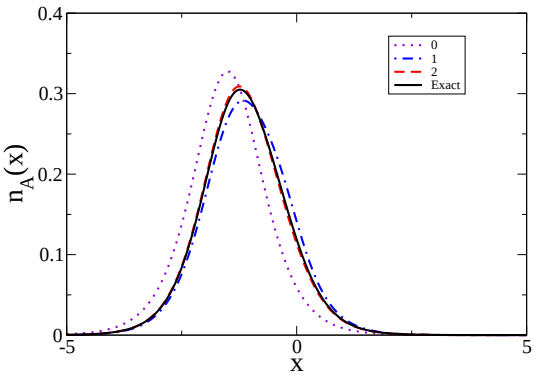

Figure 4.10: The density for the left (A) fragment as defined by Eq. (4.20) with $R = 3$ for the first 3 self-consistency cycles, labelled $0, 1, 2$ respectively. Also shown is the exact fragment density. Even after just 2 cycles, the fragment density is almost on top of the exact density, on this scale. For more self-consistency steps, it continues converging towards the exact answer. Calculations were performed using 3-site finite difference formulas for derivatives and 2001 grid points with a grid spacing of 0.013a.u.

the density $n_\alpha(x)$ and the occupation N_α. As described above, we find self-consistent solutions for fixed values of N_α. In 4.9, we plot the molecular energy found after 3 iteration cycles for 5 occupation numbers. We can clearly see that there is a minimum at $N_A = 0.655$ and in fact, it is already extremely close to the exact molecular energy. The convergence for the other occupation numbers is very slow, but the minimum at $N_A = 0.655$ remains even after 10 iteration steps. For practical calculation the occupancy may be set on the fly, but for the purposes of this demonstration, this procedure is sufficient.

To see how the density converges for each iteration, we will use the final occupation $N_A = 0.655$ from now on. In 4.10, we show the convergence for one of the two fragment densities for this problem, through several self-consistency cycles. The total potential is the same as that shown in the lower panel of 4.7, while the two fragment potentials, $v_A(x)$ and $v_B(x)$, are given in Eq. (4.20) with $R = 3$. For the initial fragment densities(cycle 0), we use the densities for the two isolated fragments. We then use these to construct a partition potential from Eq. (4.18), which is then used to construct effective fragment potentials, $v_\alpha(x) + v_p(x)$. If we then solve for each

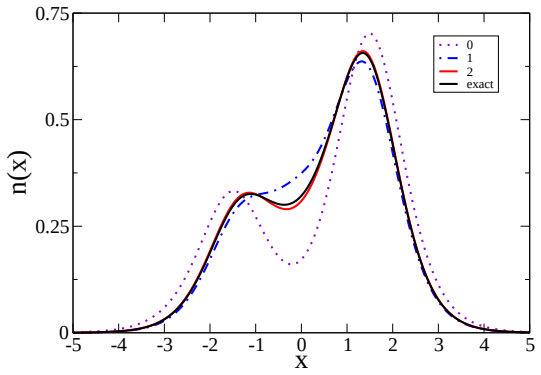

Figure 4.11: Molecular densities for various cycles $0, 1, 2$ of the self-consistency calculation for this system. Also shown is the exact density for the full system. The density after just 2 cycles is very close to the exact density and after 3 cycles it cannot be distinguished from the exact density on this scale. Convergence continues as more cycles are added, as can seen in 4.12.

fragment density in this new potential, we find the cycle 1 density, shown as the dot-dashed line in 4.10. It can be seen that the density for this fragment has been shifted towards the other 'nucleus', as compared to the isolated case. This is due to the partition potential lowering the fragment potential, v_A, so as to move density into the bonding region, as would be expected.

In 4.11, the solid line is the total molecular density, found by directly solving for two non-interacting fermions in total potential $v(x)$. It is the same as that shown in 4.7. In both this case and for the fragments, the density is found by solving the Schrödinger equation numerically on a real-space grid. Derivatives of the density are found using a finite-difference scheme. If we sum the A fragment density shown in 4.10 with its counterpart on B at each iteration step, we find the corresponding molecular density. These are plotted in 4.11 and it can be seen that the density at each self-consistency cycle is converging to the exact answer. The convergence towards the exact molecular density can be seen more clearly in 4.12 where we show the density differences from the overlapped 'atomic' densities. We add in the results for more iteration steps and

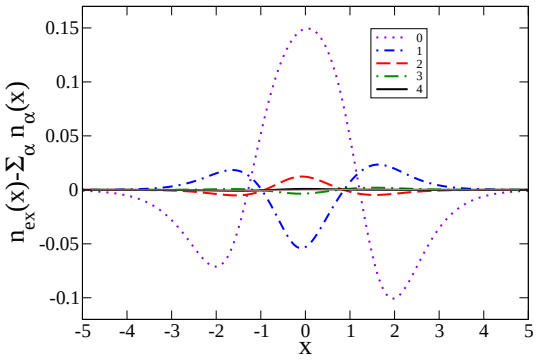

Figure 4.12: Difference between the exact molecular density, $n_{\rm ex}(x)$, and the sum of the fragment densities for each self-consistency cycle of the PDFT calculation. It is the difference between each of the PDFT densities in 4.11 and the exact density. After each cycle this difference decreases and the convergence to the exact answer is clear.

it is clear that the error decreases with every iteration.

The energy of the molecule may also be calculated using Eq. (4.9) for each set of fragment densities. Again we see the calculation converge to the exact energy of -1.30106. The energy of the initial guess was -1.26067, while after 3 cycles, it was -1.30104, essentially converged for this level of calculation .

4.5 Metal Chain

In Eq. (4.16), $v_{\rm S}[n_\alpha](\mathbf{r})$ is simply the KS fragment potential from the previous iteration, but $v_{\rm S}[n](\mathbf{r})$ is the KS potential for a trial density for the whole molecule. Many methods exist for finding this[74, 75, 76, 77, 78, 79]. We iterate[80]:

$$v_{\rm S}^{(m+1)}(\mathbf{r}) = v_{\rm S}^{(m)}(\mathbf{r}) + \gamma\left[n^{(m)}(\mathbf{r}) - n^{(k)}(\mathbf{r})\right], \tag{4.21}$$

where $n^{(m)}(\mathbf{r})$ is the density found from potential $v_{\rm S}^{(m)}(\mathbf{r})$, $\gamma > 0$ is a constant, and $n^{(k)}(\mathbf{r})$ is the target density (sum of fragment densities from the k'th PDFT iteration)

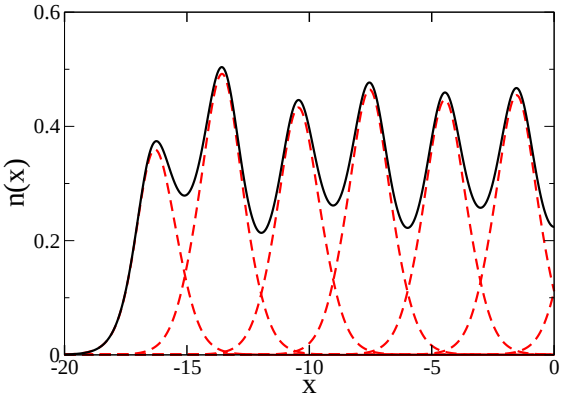

Figure 4.13: Solid line: The exact spin-unpolarized ground state of 12 electrons in the potential of Eq. (4.22). Dashed lines: The fractionally occupied fragment densities. By symmetry, the o age of that shown.

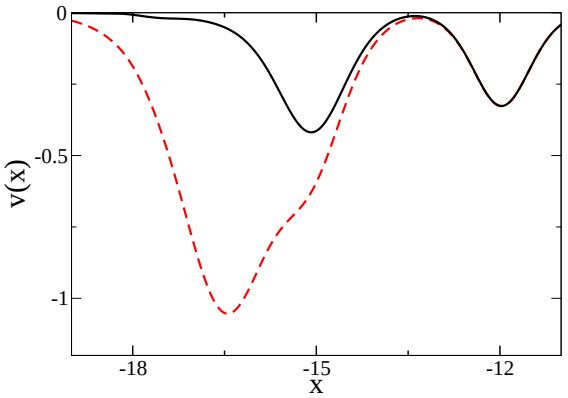

Figure 4.14: The exact partition potential (solid line) for the atomized chain and the fragment potential for the last atom (dashed line). The ground state with an occupation of 0.77 in this potential can be seen as the end fragment density in Fig 1.

whose KS potential we are trying to find. As noted previously, the fragment occupations are found using the chemical potentials, using $N_\alpha^{(k+1)} = N_\alpha^{(k)} - \Gamma\left(\mu_\alpha^{(k)} - \bar{\mu}^{(k)}\right)$, where Γ is a positive constant and $\bar{\mu}$ is the average of the fragment chemical potentials.

Note that this use of the inversion algorithm can also be useful (possibly more useful) for pure PT, to find $v_p(\mathbf{r})$ for a known $n(\mathbf{r})$. Replace $v_{\rm s}(\mathbf{r})$ by $v_p(\mathbf{r})$ in Eq. (4.21), $n^{(k)}(\mathbf{r})$ is the fixed molecular density, and $n_f^{(n)}(\mathbf{r})$ is the sum of fragment densities found from individual calculations on the fragments using $v_p^{(n)}(\mathbf{r})$ to construct the fragment potentials.

To show that our algorithm converges, we performed a PDFT calculation on a 12-atom 1d chain with 12 spin-unpolarized non-interacting fermions, with potential:

$$v(x) = \sum_{\alpha=1}^{12} \frac{-1}{\cosh^2[x + (\alpha - 6.5)R]}. \tag{4.22}$$

We chose complete atomization into 12 fragments, so we only ever solve one- or two-electron problems in a single well. Fig. 4.13 shows the atomic and molecular densities after convergence. The molecular density is identical to that found by direct solution of the eigenvalue problem for the entire molecule, and doubly occupying the first 6 eigenstates, which are delocalized over the entire molecule. We see a small alternation between higher and lower densities throughout the molecule. The fragment density occupations reflect this, being 0.77,1.13,0.98,1.06,1.02,1.04 moving inwards towards the center of the chain. In Fig. 4.14, we show both the partition potential and effective fragment potential for the last atom. The (not very large) $v_p(\mathbf{r})$ polarizes the density toward the molecular center, and shifts the density inwards compared to a free atom. The partition potential continues throughout the whole chain, lowering each fragment potential in the bonding region between atoms. The depth of these troughs oscillates, reflecting the oscillation in occupations. In Fig. 4.15, we show the convergence of the occupation numbers to their final values, after some initial oscillations. The total energy of the molecular system can be found via Eq. (4.9). We find $E_f = -5.888$ and $E_p = -1.803$ leading to $E = -7.691$, which is exactly that of the direct solution. Since $E_f^{(0)}$ is -6, $|E_{rel}| \ll |E_p| \ll |E|$, as expected.

Our calculation was in fact far more expensive than a regular KS calculation, because we invert the KS problem for each trial molecular density *exactly*. But the purpose here was not speed, but the calculation of exact partition potentials for small molecules and simple solids. It produces the *exact* partition potential corresponding to a given KS calculation for the molecule.

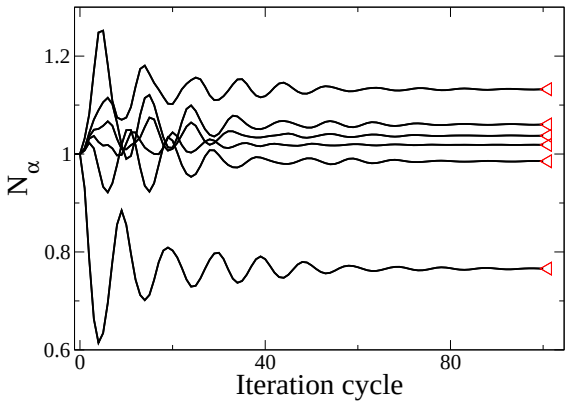

Figure 4.15: The convergence of the fragment occupation values, N_α, during an exact PDFT calculation.

4.6 Significance

We have demonstrated that with an explicit expression for the energy functional E_p, a self-consistent PDFT calculation can be performed, on fragments, and the result converges to the molecular answer. The fragments are solved individually, which, for interacting systems, would greatly reduce computational cost.

The many potential uses of PDFT are made clear by this example. In principle, Eq. (4.16) is exact, but requires the KS potential of the entire system and to deduce the energy at the end of the calculation, one needs

$$E_p = \Delta T_{\rm S}[n_\alpha] + \Delta E_{\rm HXC}[n_\alpha] + \sum_{\alpha,\beta\neq\alpha}^{N_f} \int d^3r\, n_\alpha(\mathbf{r}) v_\beta(\mathbf{r}), \tag{4.23}$$

where $\Delta G[n_\alpha] = G[\sum n_\alpha] - \sum G[n_\alpha]$. However, any local-type approximation makes the method $O(N)$. Thus, all the attempts of orbital-free DFT, to find useful approximations to $\Delta T_{\rm S}[n]$, have now a simple framework in which to be tested[81]. Moreover, there are no formal difficulties arising from taking density variations within a fixed density, as the trial molecular density is simply the sum of the fragment densities, which are varied freely. Although the exact fragment $T_{\rm S}$ and $v_{\rm S}(\mathbf{r})$ would be known

during a calculation, approximations for $\Delta T_{\rm S}$ would take full advantage of any cancellation of errors. For embedding calculations, a simple approximation would be to treat the system plus some fraction of its environment (a border region) exactly, and all the rest approximately. Since the KS potential is typically near-sighted, such a scheme should converge rapidly.

For the dissociation of molecules, one can also see how to ensure correct dissociation energies within PDFT: simply constrain occupations to be those of the isolated fragments. For H_2, we constrain the spin occupations on the fragments to be (0,1) and vice versa. Of course, this is what happens when symmetry is broken as the bond is stretched, and the difficulty is in producing a scheme that seamlessly goes over to (1/2,1/2) occupations as R reduces to the equilibrium value. The value of our formalism is that it produces a framework for both addressing these questions and constructing approximate solutions.

There is a simple adiabatic connection formula for PDFT. Consider scaling all bond lengths between fragments by λ^{-1} (again keeping intrafragment densities fixed), where $0 < \lambda \leq 1$. For each λ, we find those molecular densities whose fragment densities match those of our molecule, and define the corresponding partition energy, $E_p(\lambda)$. At $\lambda = 1$, we have the original molecule; as $\lambda \to 0$, the bonds become large and the fragments do not interact, so that $E_p(0) = 0$. For intermediate λ, the molecular density is simply that of the fragments, overlapped a distance R/λ apart. Then

$$E = E_f + \int_0^1 d\lambda \, \frac{dE_p(\lambda)}{d\lambda}. \tag{4.24}$$

This allows all the methods of traditional intermolecular symmetry-adapted perturbation theory (SAPT)[82] to be applied to this problem, but with the advantage that the fragment densities remain fixed. Interestingly, because the fragments will

generally have dipole moments, the partition energy decays as $1/R^3$, so that the integrand above behaves as λ^2. (For physical systems that are well-separated and have attractive van der Waals forces, such effects must be cancelled by analogous terms in E_{rel}).

There has been considerable previous work on schemes designed to allow a fragment calculation of a larger molecule, either within the framework of orbital-free DFT or atomic deformation potentials, sometimes producing the same (or similar) equations. Among the earliest, Cortona's crystal potential (later called embedding potential)[83, 90] is an intuitive prescription for $v_p(\mathbf{r})$. But our formalism reproduces the *exact* solution of the original problem, using only quantities that are already defined in KS-DFT. For example, this is not possible in general without the ensemble definition of Eq. (4.5), which produces the correct self-consistent occupations (unlike, e.g., the self-consistent atomic deformation method[84, 85], where this choice leads to a basis set dependence[86]) . We also never freeze the total density[87, 88, 89], but only ever consider it as a sum of fragment densities. This avoids ever needing density variations that are limited by some frozen total density, which produces bizarre functional derivatives, different from those of KS DFT. None of these issues arise once smooth (e.g. local or gradient-corrected) approximations are made to the kinetic energy functional[83, 90, 85], but they are vital in a formally exact theory. Thus the present PDFT can be regarded as a formal exactification (and therefore justification) of these pioneering works.

Chapter 5

Conclusion

In this work I have discussed two new approaches to the electronic structure problem. Both these approaches share the same goal of making electronic structure calculations faster and more accurate.

The first is potential functional theory which used semiclassical methods to find direct expressions for the density and kinetic energy density as functionals of the potential. These expressions were derived for an arbitrary potential in a box with hard walls and with no turning points at the Fermi energy, which although quite primitive already provides us with much insight. Extending this approach to the more general case that involves turning points is part of ongoing work, as is the possibility of extending it to three dimensional systems. If this were to be done, it could be used to massively speed up DFT using the scheme investigated in Ref. [91]. In any case, the main motivation behind the area of potential functional theory is to understand and improve DFT. This work allows us to explain why local approximations like Thomas-Fermi or LDA exchange work so well, namely they are the dominate terms in the semiclassical limit. We can also see why gradient corrections like GEA fail to the improve upon local

approximations as they miss the important quantum oscillation corrections. It also explains why generalized gradient approximations had to be developed before DFT became accurate enough for chemistry, and allowed us to provide an *ex post facto* derivations of the previously empirical B88 GGA exchange functional. It may also be possible to fix the GEA by including these quantum corrections.

The second approach is partition density functional theory whereby the electronic structure of a system can be found by performing calculations on smaller fragments making up the system. Due to the scaling of computational time with system size for current electronic structure methods, working on smaller pieces would greatly speed up such calculations. Unfortunately this speed up comes at the price of having to approximate more unknown pieces as a density functionals, however there is good reason to believe that the quantities involved may be quite amenable to approximation. PDFT may also help solve the problem DFT suffers from when dissociating atoms as the unknown partition energy $E_p[n]$ must vanish in this limit, making it easier to approximate.

It is interesting to speculate how the two approaches may influence eachother. In PDFT, the most difficult term to approximate is $\Delta T_{\rm S}[n]$, the difference between the molecular kinetic energy and the fragment kinetic energies as a density functional. From test calculations and experience, I expect that local or semi-local approximations will not be enough to capture this difference, and it is mainly this difference that causes the dip in the partition potential in a bonding region. However the kinetic energy in an evanescent region between two atoms is exactly the kind of quantity PFT allows us to find. Another interesting feature of PDFT is that different methods could be used on the different fragments, so PDFT gives the exact prescription on how to perform a QM/MM-like calculation. If in the eventually the density as a potential functional is not accurate enough for chemical purposes, then it still may be

a cheap way to include quantum effects in a border region or solvation, PDFT would be the correct tool to make use of this.

Bibliography

[1] *Inhomogeneous electron gas*, P. Hohenberg and W. Kohn, Phys. Rev. **136**, B 864 (1964).

[2] *Self-consistent equations including exchange and correlation effects*, W. Kohn and L.J. Sham, Phys. Rev. **140**, A 1133 (1965).

[3] *An Undulatory Theory of the Mechanics of Atoms and Molecules*, E. Schrödinger, Phys. Rev. **28**, 1049 (1926).

[4] *Semiclassical approximations in wave mechanics*, M. V. Berry and K. E. Mount, Rep. Prog. Phys. bf 35, 315 (1972).

[5] *A Primer in Density Functional Theory*, ed. C. Fiolhais, F. Nogueira, and M. Marques (Springer-Verlag, NY, 2003).

[6] see dft.uci.edu

[7] *Excited states from time-dependent density functional theory*, P. Elliott, F. Furche, and K. Burke, in Reviews in Computational Chemistry, eds. K. B. Lipkowitz and T. R. Cundari, (Wiley, Hoboken, NJ, 2009), pp 91-165.

[8] *Generalized gradient approximation made simple*, J.P. Perdew, K. Burke, and M. Ernzerhof, Phys. Rev. Lett. **77**, 3865 (1996); **78**, 1396 (1997) (E).

[9] *Density-functional exchange-energy approximation with correct asymptotic behavior*, A. D. Becke, Phys. Rev. A **38**, 3098 (1988).

[10] *Development of the Colle-Salvetti correlation-energy formula into a functional of the electron density*, C. Lee, W. Yang, and R. G. Parr, Phys. Rev. B **37**, 785 (1988).

[11] *Density-functional thermochemistry. III. The role of exact exchange*, A.D. Becke, J. Chem. Phys. **98**, 5648 (1993).

[12] *Jacobs Ladder of Density Functional Approximations for the Exchange-Correlation Energy*, J. P. Perdew and K. Schmidt, in *Density Functional Theory and Its Applications to Materials*, eds. V. E. Van Doren, K. Van Alsenoy, and P. Geerlings (American Institute of Physics, Melville, NY, 2001).

[13] *Kohn-Sham exchange potential exact to first order in* $\rho(\mathbf{K} \to 0)/\rho_0$, P.R. Antoniewicz and L. Kleinman, Phys. Rev. B **31**, 6779 (1985).

[14] *Correlation energy of an electron gas with a slowly varying high density*, S.-K. Ma and K. A. Brueckner, Phys. Rev. **165**, 18 (1968).

[15] *Density functional calculations of molecular bond energies*, A. D. Becke, J. Chem. Phys. **84**, 4524 (1986).

[16] *Static dielectric response of the electron gas*, C. Bowen, G. Sugiyama, and B. J. Alder, Phys. Rev. B **50**, 14838 (1994).

[17] *Static Response and Local Field Factor of the Electron Gas*, S. Moroni, D. M. Ceperley, and G. Senatore, Phys. Rev. Lett. **75**, 689 (1995).

[18] *Improved lower bound on the indirect Coulomb energy*, E. H. Lieb and S. Oxford, Int. J. Quantum Chem. **19**, 427 (1981).

[19] *The calculation of atomic fields*, L.H. Thomas, Proc. Camb. Phil. Soc. **23**, 542 (1926).

[20] *A statistical method for the determination of some atomic properties and the application of this method to the theory of the periodic system of elements* E. Fermi, Zeit. Fur Physik **48**, 73 (1928).

[21] The Thomas-Fermi approximation in quantum mechanics N. H. March, Adv. in Phys. **6**, 1 (1957).

[22] *Thomas-Fermi model: The leading correction*, J. Schwinger, Phys. Rev. A **22**, 1827 (1980); *Thomas-Fermi model: The second correction*, ibid. **24**, 2353 (1981).

[23] *Quantum corrections to the Thomas-Fermi equation*, D.A. Kirzhnits, Sov. Phys. JETP **5**, 64 (1957).

[24] *Generalized gradient approximation for solids and their surfaces*, J. Perdew, A. Ruzsinszky, G.I. Csonka, O.A. Vydrov, G.E. Scuseria, L.A. Constantin, X. Zhou, and K. Burke, arXiv:0707:2088

[25] *Potential Functionals: Dual to Density Functionals and Solution to the v-Representability Problem*, W. Yang, P.W. Ayers, and Q. Wu, Phys. Rev. Lett. **92**, 146404 (2004)

[26] *Thomas-fermi and related theories of atoms and molecules*, E.H. Lieb, Rev. Mod. Phys. **53**, 603 (1981).

[27] *Hellmann-Feynman, virial, and scaling requisites for the exact universal density functionals. Shape of the correlation potential and diamagnetic susceptibility for atoms*, M. Levy and J.P. Perdew, Phys. Rev. A **32**, 2010 (1985).

[28] *A new chemical concept: Shape chemical potentials*, G.K.L. Chan and N.C. Handy, J. Chem. Phys. **109**, 6287 (1998).

[29] *Relevance of the slowly-varying electron gas to atoms, molecules, and solids*, J. P. Perdew, L. A. Constantin, E. Sagvolden, and K. Burke, Phys. Rev. Lett. **97**, 223002 (2006).

[30] *Recursion representation of gradient expansion for free fermion ground state in one dimension*, L. Samaj and J.K Percus, J. Chem. Phys. **111**, 1809 1999.

[31] *Quantum density oscillations in an inhomogeneous electron gas*, W. Kohn and L. Sham, Phys. Rev. **137**, A1697 (1965).

[32] *Density-functional exchange-correlation through coordinate scaling in adiabatic connection and correlation hole*, M. Levy, Phys. Rev. A **43**, 4637 (1991).

[33] *Tight bound and convexity constraint on the exchange-correlation-energy functional in the low-density limit, and other formal tests of generalized-gradient approximations*, M. Levy and J.P. Perdew, Phys. Rev. B **48**, 11638 (1993); ibid., **55**, 13321 (1997)(E).

[34] *Nonuniform coordinate scaling requirements for exchange-correlation energy*, M. Levy and H. Ou-Yang, Phys. Rev. A **42**, 651 (1990).

[35] *Exchange-correlation energy of a metallic surface: Wave-vector analysis*, D.C. Langreth and J.P. Perdew, Phys. Rev. B **15**, 2884 (1977).

[36] *Theory of nonuniform electronic systems. I. Analysis of the gradient approximation and a generalization that works*, D.C. Langreth and J.P. Perdew, Phys. Rev. B **21**, 5469 (1980).

[37] *The surface energy of a bounded electron gas*, J. Harris and R.O. Jones, J. Phys. F **4**, 1170 (1974).

[38] *Exchange and correlation in atoms, molecules, and solids by the spin-density-functional formalism*, O. Gunnarsson and B.I. Lundqvist, Phys. Rev. B **13**, 4274 (1976).

[39] *Some remarks on scaling relations in density functional theory*, W. Yang, in *Density Matrices and Density Functionals*, eds. R. Erdahl and V. H. Smith, Jr. (D. Reidel Publishing Company, Dordrecht, The Netherlands, 1987), pp 499-506.

[40] *A new functional with homogeneous coordinate scaling in density functional theory: F[ρ,λ]*, M. Levy, W. Yang, and R. G. Parr, J. Chem. Phys. **83**, 2334 (1985).

[41] *Rationale for mixing exact exchange with density functional approximations*, J.P. Perdew, M. Ernzerhof, and K. Burke, J. Chem. Phys. **105**, 9982 (1996).

[42] *The adiabatic connection method: A non-empirical hybrid*, K. Burke, M. Ernzerhof, and J.P. Perdew, Chem. Phys. Lett. **265**, 115 (1997).

[43] *Mixing exact exchange with GGA: When to say when*, K. Burke, J.P. Perdew, and M. Ernzerhof, in *Electronic Density Functional Theory: Recent Progress and New Directions*, eds. J.F. Dobson, G. Vignale, and M.P. Das (Plenum, NY, 1998), page 57.

[44] *Construction of the adiabatic connection*, M. Ernzerhof, Chem. Phys. Lett. **263**, 499 (1996).

[45] *Generalized gradient approximation for solids and their surfaces*, J. Perdew, A. Ruzsinszky, G.I. Csonka, O.A. Vydrov, G.E. Scuseria, L.A. Constantin, X. Zhou, and K. Burke, Phys. Rev. Lett. **100**, 136406 (2008).

[46] *Adiabatic connection from accurate wavefunction calculations*, D. Frydel, W. Terilla, and K. Burke, J. Chem. Phys. **112**, 5292 (2000).

[47] *Comparison of approximate and exact density functionals: A quantum monte carlo study*, C.J. Umrigar and X. Gonze, in *High Performance Computing and its Application to the Physical Sciences*, Proceedings of the Mardi Gras 1993 Conference, edited by D. A. Browne et al. (World Scientific, Singapore, 1993).

[48] *Accurate exchange-correlation potentials and total-energy components for the helium isoelectronic series*, C.J. Umrigar and X. Gonze, Phys. Rev. A **50**, 3827 (1994).

[49] *Thomas-Fermi Theory Revisited*, E.H. Lieb and B. Simon, Phys. Rev. Lett. **31**, 681 (1973).

[50] *Semiclassical Origins of Density Functionals*, P. Elliott, D. Lee, A. Cangi, and K. Burke, Phys. Rev. Lett. **100**, 256406 (2008).

[51] OPMKS: atomic DFT program, University of Frankfurt, Germany., E. Engel

[52] *Local correlation energies of two-electron atoms and model systems*, C.J. Huang and C.J. Umrigar, Phys. Rev. A **56**, 290 (1997).

[53] *Exact Condition on the Kohn-Sham Kinetic Energy, and Modern Parametrization of the Thomas-Fermi Density*, D. Lee, K. Burke, L.A. Constantin, J.P. Perdew, submitted to J. Chem. Phys. (Fall 2008).

[54] *Semiclassical theory of atoms*, B.-G. Englert, Lect. Notes Phys. **300** (1988).

[55] *Sixth-order term of the gradient expansion of the kinetic-energy density functional*, D. R. Murphy, Phys. Rev. A **24**, 1682 (1981).

[56] *Numerical test of the sixth-order gradient expansion for the kinetic energy: Application to the monovacancy in jellium*, Z. D. Yan, J. P. Perdew, T. Korhonen, and P. Ziesche, Phys. Rev. A **55**, 4601 (1997).

[57] *Exchange and correlation energy in a nonuniform fermion fluid*, M. Rasolt and D. J. W. Geldart, Phys. Rev. B **34**, 1325 (1986).

[58] *Density-functional thermochemistry. III. The role of exact exchange*, A. D. Becke, J. Chem. Phys. **98**, 5648 (1993).

[59] *Thomas-Fermi model: The leading correction*, J. Schwinger, Phys. Rev. A **22**, 1827 (1980); *Thomas-Fermi model: The second correction*, ibid. **24**, 2353 (1981).

[60] *Semiclassical atom*, B.-G. Englert and J. Schwinger, Phys. Rev. A **32**, 26 (1985).

[61] C. Froese-Fischer, *The Hartree-Fock method for atoms: a numerical approach* (Wiley, New York, 1977).

[62] *Condition on the Kohn-Sham Kinetic Energy, and Modern Parametrization of the Thomas-Fermi Density*, D. Lee, L. A. Constantin, J. P. Perdew, and K. Burke, J. Chem. Phys. **130**, 034107 (2009).

[63] *Unified theory of exchange and correlation beyond the local density approximation*, J. P. Perdew, in *Electronic Structure of Solids 91*, eds. P. Ziesche and H. Eschrig (Akademie Verlag, Berlin, 1991), pp. 11.

[64] *Derivation of a generalized gradient approximation: The PW91 density functional*, K. Burke, J. P. Perdew, and Y. Wang, in *Electronic Density Functional Theory: Recent Progress and New Directions*, eds. J. F. Dobson, G. Vignale, and M. P. Das (Plenum, NY, 1998), pp. 81.

[65] R. M. Dreizler and E. K. U. Gross, Density Functional Theory (Springer-Verlag, Berlin, 1990).

[66] *The wave mechanics of an atom with a non-coulomb central field I. Theory and methods*, D. R. Hartree, Proc. Cambridge Phil. Soc. **24**, 89 (1928).

[67] *Näherungsmethode zur Losung des quantenmechanischen Mehrkörperprobleme*, V. Fock, Z. Phys. **61**, 126 (1930).

[68] Peter Fulde, *Electron Correlations in Molecules and Solids* (Springer-Verlag, Berlin, 1991).

[69] *On the foundations of Chemical Reactivity Theory*, M. H. Cohen and A. Wasserman, J. Phys. Chem. A **111**, 2229 (2007).

[70] *On hardness and electronegativity equalization in Chemical Reactivity Theory*, M. H. Cohen and A. Wasserman, J. Stat. Phys. **125**, 1125 (2006).

[71] *Density-functional theory for fractional particle number: Derivative discontinuities of the energy*, J. P. Perdew, R.G. Parr, M. Levy, and J.L. Balduz, Jr., Phys. Rev. Lett. **49**, 1691 (1982).

[72] *What do the Kohn-Sham orbitals mean? How do atoms dissociate?*, J.P. Perdew, in *Density Functional Methods in Physics*, edited by R.M. Dreizler and J. da Providencia (Plenum, NY, 1985), p. 265.

[73] *Charge Transfer in Partition Theory*, M. H. Cohen, A. Wasserman, R. Car, and K. Burke, J. Phys. Chem. A **113**, 2183 (2009).

[74] *Kohn-Sham method as a free-energy minimization at infinite temperature*, R.G. Parr and Y.A. Wang, Phys. Rev. A **55**, 3226 (1997).

[75] *From electron densities to Kohn-Sham kinetic energies, orbital energies, exchange-correlation potentials, and exchange-correlation energies*, Q. Zhao, R.C. Morrison, and R.G. Parr, Phys. Rev. A **50**, 2138 (1994).

[76] *On the Optimal Mixing of the Exchange Energy and the Electron-Electron Interaction Part of the Exchange-Correlation Energy*, O. Gritsenko, R. van Leeuwen, and E.J. Baerends, Int. J. Quantum Chem. **30**, 1375 (1996).

[77] *A direct optimization method for calculating density functionals and exchange-correlation potentials from electron densities*, Q. Wu and W. Yang, J. Chem. Phys. **118**, 2498 (2003).

[78] *Correlation energies for some two- and four-elactron systems along the adiabatic connection in density functional theory*, F. Colonna, A. Savin, J. Chem. Phys. **110**, 2828 (1999).

[79] *Separation of the exchange-correlation potential into exchange plus correlation: An optimized effective potential approach*, C. Filippi, C.J. Umrigar, and X. Gonze, Phys. Rev. A **54**, 4810 (1996).

[80] *Algorithm to derive exact exchange-correlation potentials from correlated densities in atoms*, K. Peirs, D. Van Neck, and M. Waroquier, Phys. Rev. A **67**, 012505 (2003).

[81] *The energy-differences based exact criterion for testing approximations to the functional for the kinetic energy of non-interacting electrons*, Y. A. Bernard, M. Dulak, J. W. Kaminski, T. A. Wesolowski, J. Phys. A: Math. Theor. **41**, 055302 (2008).

[82] *Dispersion Energy from Density-Functional Theory Description of Monomers*, A. J. Misquitta, B. Jeziorski, and K. Szalewicz, Phys. Rev. Lett. **91**, 033201 (2003).

[83] *Self-consistently determined properties of solids without band-structure calculations* P. Cortona, Phys. Rev. B **44**, 8454 (1991).

[84] *Self-consistent deformation method for application of density functional theory* L. L. Boyer, H.T. Stokes, M.M. Ossowski, and M.J. Mehl, Phys. Rev. B **78**, 045121 (2008).

[85] Development of a Kohn-Sham like potential in the self-consistent atomic deformation model M.J. Mehl, H.T. Stokes, and L.L. Boyer, J. Phys. Chem. Solids **57**, 1405 (1996).

[86] *Water molecule by the self-consistent atomic deformation method*, M. M. Ossowski, L. L. Boyer, M. J. Mehl, and M. R. Pederson, Phys. Rev. B **68**, 245107 (2003).

[87] *Frozen density functional approach for ab inition calculations of solvated molecules* T.A. Wesolowski and A. Warshel, J. Phys. Chem. A **97**, 8050 (1993).

[88] *Electronic-structure calculations by first-principles density-based embedding of explicitly correlated systems* N. Govind, Y.A. Wang, and E.A. Carter, J. Chem. Phys. **110**, 7677 (1999).

[89] *Self-consistent embedding theory for locally correlated configuration interaction wave functions in condensed matter* P. Huang, and E.C. Carter, J. Chem. Phys. **125**, 084102 (2006).

[90] *Direct determination of self-consistent total energies and charge densities of solids: A study of the cohesive properties of the alkali halides* P. Cortona, Phys. Rev. B **46**, 2008 (1992).

[91] *Adiabatic Connection and the KohnSham Variety of PotentialFunctional Theory*, E. K. U. Gross and C. R. Proetto, J. Chem. Theory Comput. **5**, 844 (2009).

Appendices

A Exchange energy for non-interacting Beryllium

The limit of the inequality, Eq. (3.56), is the Hartree-exchange functional evaluated on the density of the corresponding non-interacting system. Since the g.s. orbitals which sum to this density are known analytically (they are simply hydrogenic orbitals), we may calculate the exact Hartree-exchange value.

Written in spherical coordinates, $r = |\mathbf{r}|$, the $1s$ and $2s$ hydrogenic orbitals are:

$$\phi_{1s}(\mathbf{r}) = \left(\frac{Z^3}{\pi}\right)^{1/2} e^{-Zr} , \tag{A.1}$$

$$\phi_{2s}(\mathbf{r}) = \left(\frac{Z^3}{32\pi}\right)^{1/2} (2 - Zr)e^{-Zr/2} . \tag{A.2}$$

For beryllium, both these orbitals are doubly occupied, giving the total density as

$$n(\mathbf{r}) = 2|\phi_{1s}(\mathbf{r})|^2 + 2|\phi_{2s}(\mathbf{r})|^2 . \tag{A.3}$$

The Hartree energy is defined by Eq. (2.42), however in the special case of spherical

densities it may be written as:

$$U[n] = \frac{1}{2}\int_0^\infty dr \ \ (f[n](r))^2 \ , \tag{A.4}$$

where

$$f[n](r) = 4\pi \int_r^\infty dr' \ r'n(r') \ , \tag{A.5}$$

and we use square brackets to indicate that it is a functional of the density. The exchange energy for a spin-unpolarized system is:

$$E_{\rm X} = -2\frac{1}{2}\sum_{i,j}^{occ} \int d^3r \int d^3r' \ \frac{\phi_i^*(\mathbf{r})\phi_j^*(\mathbf{r}')\phi_j(\mathbf{r})\phi_i(\mathbf{r}')}{|\mathbf{r}-\mathbf{r}'|} \ , \tag{A.6}$$

where the factor 2 is due to spin, and the sum is over occupied orbitals only, in this case $1s$ and $2s$. If we define a new quantity, $\tilde{n}(\mathbf{r})$:

$$\tilde{n}(\mathbf{r}) = \phi_{1\rm s}(\mathbf{r})\phi_{2\rm s}(\mathbf{r}) \ , \tag{A.7}$$

then we may write

$$E_{\rm X} = -2\left(U[n_{1\rm s}] + 2U[\tilde{n}] + U[n_{2\rm s}]\right) \ . \tag{A.8}$$

We can use Eq. (A.5) and Eq. (A.4) for each term separately and then combine to find the total exchange energy. The answer will be equivalent to solving Eq. (A.6) using the orbitals, however this method avoids performing integrals involving $1/|\mathbf{r}-\mathbf{r}'|$ and, in this case, are easy to solve using integration by parts. The values for Hartree, exchange and their sum are:

$$U[n] = \frac{5\times 23\times 431}{2^6 3^4} = \frac{49565}{5184} = 9.561 \ ,$$

$$E_{\rm X} = -\frac{59 \times 71 \times 73}{2^7 3^6} = -\frac{305797}{93312} = -3.277 \ ,$$

$$E_{\rm HX} = \frac{383 \times 1531}{2^7 3^6} = \frac{586373}{93312} = 6.284 \ .$$

B Finding $E_{\rm F}$

Solving the quantization condition for the Fermi energy:

$$\theta_{\rm F}(L) = \int_0^L dx \ k_{\rm F}(x) = (N + 0.5)\pi \tag{B.9}$$

can be done via a Newton-like method. An initial guess for $\epsilon_{\rm F}$ is made, usually the flat box value:

$$\epsilon_{\rm F}^g = \left[\frac{(N + 1/2)\pi}{L}\right]^2$$

This will differ from the correct $\epsilon_{\rm F}$ by $\Delta\epsilon$, which we will assume to be small. Then we can expand Eq. (B.9) as

$$\theta_1(L, \epsilon_{\rm F}^g) + \frac{\Delta\epsilon}{2}\tau_1(L, \epsilon_{\rm F}^g) = (N + 1/2)\pi \tag{B.10}$$

thus $\Delta\epsilon$ may be calculated. This can be added to the first initial guess $\epsilon_{\rm F}^g$ to find a new initial guess and the process repeated until $\epsilon_{\rm F}$ is found to the accuracy required.

C Charge-neutral scaling inequality

We follow the steps in deriving Eq. (3.48) but applied to the charge neutral scaling defined in Eq. (3.42). Taking $n^{\zeta}_{1/\zeta}(\mathbf{r})$ as a trial density for the $v(\mathbf{r})$ system, then the variational principle states:

$$F[n^{\zeta}_{1/\zeta}] + V[n^{\zeta}_{1/\zeta}] \geq F[n] + V[n] \ , \tag{C.11}$$

where $n^{\zeta}(\mathbf{r})$ is the exact density for the scaled potential $v^{\zeta}(\mathbf{r})$. Conversely, use $n_{\zeta}(\mathbf{r})$ as a trial density for the $v^{\zeta}(\mathbf{r})$ system:

$$F[n_{\zeta}] + \zeta^{7/3} V[n] \geq F[n^{\zeta}] + \zeta^{7/3} V[n^{\zeta}_{1/\zeta}] \tag{C.12}$$

where we have used $V^{\zeta}[n_{\zeta}] = \zeta^{7/3} V[n]$. Combining these inequalities gives:

$$\frac{F[n_{\zeta}] - F[n^{\zeta}]}{\zeta^{7/3}} \geq F[n] - F[n^{\zeta}_{1/\zeta}] \ , \tag{C.13}$$

which may be written as

$$\Delta F^{\zeta}[n^{\zeta}_{1/\zeta}] \geq \Delta F^{\zeta}[n] \ , \tag{C.14}$$

with

$$\Delta F^{\zeta}[n] = F[n] - \frac{F[n_{\zeta}]}{\zeta^{7/3}} \ . \tag{C.15}$$